ENGINEERING
LIBRARY

JAN 27 1950

JOURNAL OF

THE INSTITUTE OF PETROLEUM

FOUNDED 1913 + INCORPORATED 1914

Vol. 35 NOVEMBER 1949 No. 311

Contents

The Evaluation of Gassing Tendencies of Insulating Oils: Apparatus, Procedure, and Effect of Experimental Variables.
By G. H. Beaven, J. A. Cockburn, C. N. Thompson.

"Knock" Tests using an Atmosphere in which Nitrogen is Replaced by Argon and Carbon Dioxide.
By D. Downs and J. H. Pignéguy.

Adiabatic and Non-Adiabatic Rectification.
By Kuo-tsung Yu and James Coull.

The Shell-Ricardo Lubricating-Oil Test Engine.
By D. Downs.

Calibration of I.P. Diesel Reference Fuels H.I.Q. and L.I.Q. in Terms of Cetane Number.

Abstracts.

Book Reviews.

Applications for Membership or Transfer.

Published by the Institute of Petroleum,
Address: Manson House, 26 Portland Place, London, W.1.
Telephone No.: LANgham 2250.
Telegraphic Address: Instpetech, Westdo, London.
Printed in Great Britain by Richard Clay and Company, Ltd., Bungay, Suffolk.

Price 7s. 6d. Annual Sub. £3 13s. 6d. (Post Free)

COUNCIL, 1948–1949

PRESIDENT:

E. A. Evans, M.I.Mech.E., F.R.I.C.

PAST-PRESIDENTS:

Sir Andrew Agnew, C.B.E.
S. J. M. Auld, O.B.E., M.C., D.Sc.
J. S. S. Brame, C.B.E., F.R.I.C.
T. Dewhurst, A.R.C.S.
A. E. Dunstan, D.Sc., F.R.I.C.
F. H. Garner, O.B.E., Ph.D., F.R.I.C.
J. Kewley, M.A., F.R.I.C.

VICE-PRESIDENTS:

M. A. L. Banks, B.Sc., F.R.I.C.
E. J. Dunstan, M.Sc.
E. B. Evans, Ph.D., M.Sc., F.R.I.C.
H. Hyams
J. S. Parker, M.A., B.Sc.
C. A. P. Southwell, M.C., B.Sc.

MEMBERS OF COUNCIL:

W. S. Ault, B.A.
V. Biske, LL.B., B.Sc., F.R.I.C.
C. D. Brewer, M.I.Mech.E
C. T. Brunner, M.A.
F. L. Garton, M.A., B.Sc.
H. S. Gibson, C.B.E., M.A., M.I.Mech.E.
T. F. Laurie
J. A. Oriel, C.B.E., M.C., M.A.
F. Morton, Ph.D., F.R.I.C.
H. E. F. Pracy, B.A.
D. L. Samuel, B.Sc., A.R.I.C.
G. H. Smith, Ph.D.
R. B. Southall
E. Stokoe
E. J. Sturgess, B.Sc.
H. C. Tett, B.Sc., D.I.C.
G. H. Thornley, M.Sc.
E. Thornton, B.Sc., F.R.I.C.
H. de Wilde, M.Sc., M.I.Mech.E.
A. T. Wilford, B.Sc., A.R.I.C.
W. J. Wilson, F.R.I.C., A.C.G.I.

EX-OFFICIO:

A. J. Goodfellow, B.Sc., A.R.I.C.
N. E. F. Hitchcock, B.Sc. } London Branch.

A. Fleming. Scottish Branch.

T. W. Ranson. Northern Branch.

E. J. Horley. South Wales Branch.

J. G. Hancock. Stanlow Branch.

HONORARY SECRETARY: C. Chilvers, B.Sc., F.R.I.C.

HONORARY TREASURER: G. H. Coxon

HONORARY EDITOR: F. H. Garner, O.B.E., Ph.D., F.R.I.C.

HONORARY ASSOCIATE EDITOR: E. B. Evans, Ph.D., M.Sc., F.R.I.C.

EDITOR: George Sell

GENERAL SECRETARY: D. A. Hough, A.I.A.C.

TECHNICAL SECRETARY: Peter Kerr, M.A., B.Sc., F.R.I.C.

LIBRARIAN: Mrs P. Steele, A.L.A.

HON. SECRETARIES OF BRANCHES

London Branch: N. E. F. Hitchcock, c/o C. C. Wakefield & Co. Ltd., Crown Works, Hayes, Middlesex.

Fawley Branch: I. McCallum, "Treside," New Road, Hythe, Southampton.

Northern Branch: G. M. Davies, c/o Anglo-American Oil Co., Mode Wheel Installations, Trafford Wharf Road, Manchester 17.

Scottish Branch: W. M. Stirling, Scottish Oils Ltd., Middleton Hall, Uphall, Broxburn, W. Lothian.

South Wales Branch: E. J. Horley, National Oil Refineries Ltd., Llandarcy, Glam.

Stanlow Branch: V. Biske, Lobitos Oilfields Ltd., The Refinery, Ellesmere Port, Cheshire.

Trinidad Branch: J. S. Collcott, B.Sc., c/o Trinidad Petroleum Development Co. Ltd., Palo Seco, via Siparia, Trinidad, B.W.I.

Vol. 35. No. 311. November 1949.

THE EVALUATION OF GASSING TENDENCIES OF INSULATING OILS: APPARATUS, PROCEDURE, AND EFFECT OF EXPERIMENTAL VARIABLES.

By G. H. Beaven, J. A. Cockburn, and C. N. Thompson.

Summary.

1. Previous work on this subject is summarized, and the observed phenomena are discussed. Experimental techniques are outlined.
2. A convenient numerical form of expressing the results of gassing tests has been introduced.
3. The effects of the following experimental variables on the results of gassing tests have been determined :—
(*a*) random supply-voltage variations; (*b*) working voltage; (*c*) temperature; (*d*) inner electrode dimensions; (*e*) position of oil-gas interface; (*f*) nature of gas phase.
4. Simple electrostatic theory has been used to calculate the radial variation of voltage gradient in the apparatus.
5. Previous explanations of the gassing process in hydrocarbon insulating oils have been applied to the present results.

Introduction.

There is a considerable volume of published work [1-16] on the decomposition of hydrocarbons under electric stress and related influences. The early workers, starting with Thenard in 1873, subjected hydrocarbon vapours to the silent electric discharge in apparatus of the ozonizer type, consisting of concentric glass tubes with the hydrocarbon contained between them, and using either metal foils or conducting liquids as the electrodes. The silent electric discharge has also been used in more recent investigations,[3, 5, 6, 11, 12, 15, 19, 20] which have been extended to include such agencies as corona [16] and semi-corona [4] discharges, glow discharges,[8, 13] α-particles,[1, 2, 9] deuterons,[9] and cathode rays.[7, 10] The distinctions made between silent, corona, semi-corona, and glow discharges appear to be of a rather arbitrary nature.

The results of experiments with discharges of various types and with charged particles show a large measure of agreement, the products of the decomposition being gases, liquids, and solid materials in varying proportions, depending largely on the chemical nature of the hydrocarbon. Hydrogen predominates in the gaseous products,[7, 10, 12, 16] and in the absence of oxygen the solid products have the composition of polymeric hydrocarbons, extending over a wide range of physical and chemical characteristics.

This brief summary of the behaviour of hydrocarbons in general applies to insulating oils of petroleum origin.[7, 10, 11, 12, 13, 16] The possibility of the decomposition of such products under electric stress is of technological importance in view of their use in oil-impregnated-paper insulation in cables and capacitors. The solid decomposition products are not necessarily harmful, except where they may impede the movements of fluid insulating oils arising from changes in operating temperatures, or diminish

the heat-transfer properties of the liquid media. The formation of bubbles of gas in laminated paper insulation, however, may result in local discharges, which involve dissipation of electrical energy as heat, leading to deterioration and eventually breakdown of the paper insulation. A further consequence of discharges in such gas bubbles is the increased exposure of the oil itself (or its vapour) to bombardment by ions produced in the discharge and accelerated by the local electric field in which the bubbles are located. Both the thermal and electrical effects are thus deleterious to the insulation in general.

The apparatus discussed here was originally devised for evaluating the relative gas-forming tendencies under electric stress of low-viscosity insulating oils for use in the Pirelli hollow-core cable. The Pirelli gassing apparatus does not appear to have been completely described in the literature, nor the relation of the information provided by it to the service conditions and performance of insulating oils discussed in any detail. It is, however, widely known to insulating-oil technologists, and has been briefly mentioned in papers by Nederbragt,[11] Wood-Mallock and Thompson,[17] and Meyer.[18]

Under these circumstances, the Pirelli gassing test has already been the subject of considerable interest by manufacturers and consumers of insulating oils. It may be more widely used in the future as a method of selecting refining procedures. For these reasons, it was considered important to study it in some detail, with a view to choosing the best design and operating procedure, assessing its accuracy and long-term reproducibility, evaluating the electrical aspects of the test and relating them to the conditions existing in cables and capacitors, and finally to relate the gassing characteristics of insulating oils to their hydrocarbon-type composition.

Experimental.

Description of the "B.P.M.-Pirelli" Apparatus and Working Procedure.

The apparatus (Fig. 1) developed by the N.V. de Bataafsche Petroleum Maatschappij (B.P.M.) Amsterdam laboratory [14] from the original Pirelli design was used without modification for the initial work at Thornton Research Centre (T.R.C.). The glass reaction vessel *A* is made of 13-mm-I.D. tubing (1 mm wall) and contains the inner electrode *B* of V_2A steel (dia 2·5 mm) which is welded to a tungsten lead wire sealed into the lower end of *A*. The external electrode *C* is of tin-foil, length 60 mm, forming one complete turn round *A* with a slight overlap. It is held in position by single turns of thin copper wire at top and bottom, and a vertical slit for observing the oil–gas interface is cut in it. A capillary tube sealed into the bottom of *A* is terminated by a three-way 120° stopcock *E* and sample reservoir. The reaction vessel is connected to the manometer *D*, made of 6-mm-I.D. tubing. A horizontal reference line (*a*) is etched on the reaction vessel at the mid-point of the outer electrode, and a similar mark (*b*) at the corresponding point on the manometer. The reaction vessel is immersed in a beaker of oil maintained at the working temperature by manual control, while the manometer is at room temperature; it is preferably surrounded by a small water jacket (Thornton practice) to prevent heating by radiation from the oil-bath.

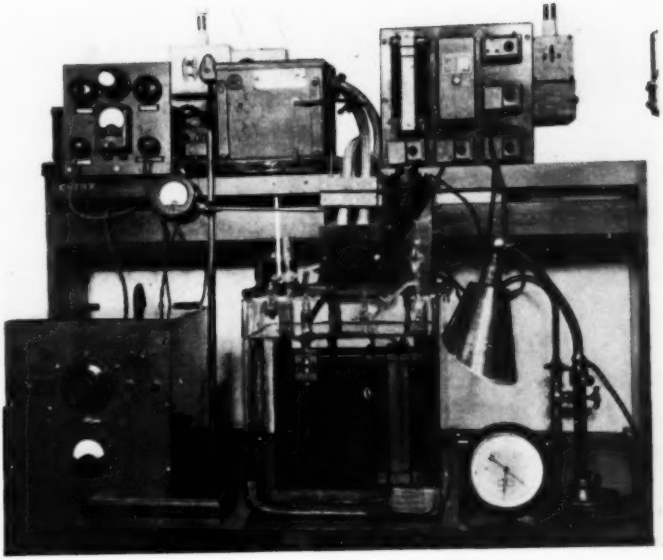

PLATE I.

MODIFIED GASSING APPARATUS : GENERAL VIEW OF APPARATUS IN THERMOSTAT READY FOR USE.

Electrical supply and thermostat controls on shelf.

[*To face p.* 736.

The working procedure is as follows. The manometer is filled to the mark (*b*) with the oil to be tested, and the sample reservoir is also filled. The apparatus is filled with hydrogen, and the oil in the manometer saturated with the same gas, introduced at *E* from a cylinder of pure electrolytic hydrogen. The stream of hydrogen through the apparatus is maintained for 10 min, then *E* is turned to divert the gas through the oil in the sample reservoir for a further 10 min. The hydrogen-saturated sample is then run into the reaction vessel up to the mark (*a*), and the internal pressure adjusted to atmospheric by venting excess hydrogen through stopcock *F*; a few drops of oil in the tube above *F* serve to prevent back-diffusion of air. After temperature equilibrium has been established

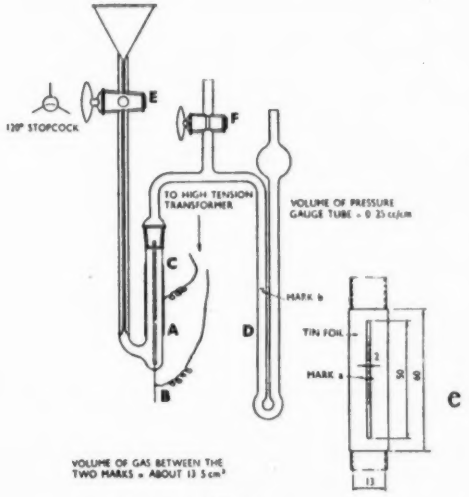

FIG. 1.

B.P.M.–PIRELLI APPARATUS FOR EXAMINING THE GAS GENERATION OF INSULATING OILS UNDER HYDROGEN PRESSURE.

(15 min) and the pressure readjusted if necessary, a voltage of 10 or 15 kV* (r.m.s.) at power frequency (50 c.p.s.) is applied to the electrodes from a suitable transformer, *e.g.*, a neon-sign pattern with an output rating of 50 mA. Manometer readings are taken at regular intervals over a period of about 100 min.

The results may be expressed graphically as plots of manometer pressure (in cm of oil) versus time (Fig. 2). Under proper working conditions such plots are normally linear, and the relative gassing tendency of an oil can be expressed in terms of the total pressure *P* developed during a fixed time, *e.g.*, 10 to 110 min (to eliminate the effect of slight irregularities in

* Except when otherwise stated all voltages in this paper are "root mean square" or "effective" values. For pure sine wave forms these are related to the "maximum" or "crest" values by the equation $V_{r.m.s.} = V_{max.}/\sqrt{2}$.

the pressure change during the first few minutes of the experiment). Alternatively, the slope S of the plot in cm of oil/min can be used. At Thornton, S has been adopted as a measure of gassing tendency, and for the majority of products examined $S \times 100$ comes within the range -20 to $+20$ with an apparatus approximating to the dimensions of Fig. 1 used at 50° C and 10 kV. (All the S values in this paper have been multiplied by 100 for convenience.) It will be evident that S is positive for gas *evolution*, negative for *absorption*, and zero if the sample neither evolves nor absorbs gas under the particular conditions used.

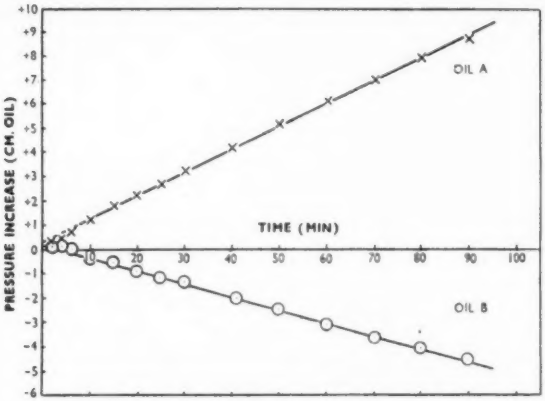

FIG. 2.

GAS EVOLUTION AND ABSORPTION OF ELECTRICAL OILS IN THE GASSING APPARATUS. Typical pressure increase *versus* time plots (original apparatus).

The gas in the apparatus remains substantially at atmospheric pressure during an experiment ($\pm$ a few cm of oil of density *ca* 0·8), so that the observed pressure change is effectively a measure of the volume of gas absorbed or evolved in terms of the volume per cm of the manometer tube. For the apparatus of Fig. 1 this is *ca* 0·28 ml/cm, and S can be converted into ml gas/min by using this factor. Such a procedure is not necessary for the comparison of results all obtained in the same apparatus.

Factors Affecting Reproducibility of Results.

The linearity of the pressure *vs* time plot was often very poor in the earlier experiments. The rate of gas evolution or absorption appeared to alter suddenly during the course of a run (Fig. 3). This effect was traced to abrupt changes in the actual voltage of the nominal 250-V supply to the primary of the high-voltage transformer due to heavy load fluctuations on the circuit. A saturated-core constant-voltage transformer between the supply and the H.V. transformer reduced these variations to ± 1 V or less.

Errors due to temperature variations were minimized by immersing the reaction vessel in an oil thermostat maintained at $50 \pm 0{\cdot}2°$ C. Under these conditions the variation in S for a given oil was not more than 7 per

cent of the mean value in consecutive experiments. The long-term reproducibility of the results, assessed by determinations on a reference oil (D) * at intervals in the course of measurements on other samples, was very much worse than the "short-term" reproducibility in consecutive tests. Thus, with one particular apparatus and oil, S fluctuated between $+8{\cdot}0$ and $+6{\cdot}0$, and eventually fell to $+5{\cdot}0$.

Examination of the reaction vessel after a large number of tests revealed a white deposit on the glass extending downwards from the oil–gas interface. Similar deposits have been noted by other workers.[7,10,12,13,16] This material, presumably similar to "cable wax" or "cheese,"[16] was evidently not removed by the conventional oil solvents used to clean the

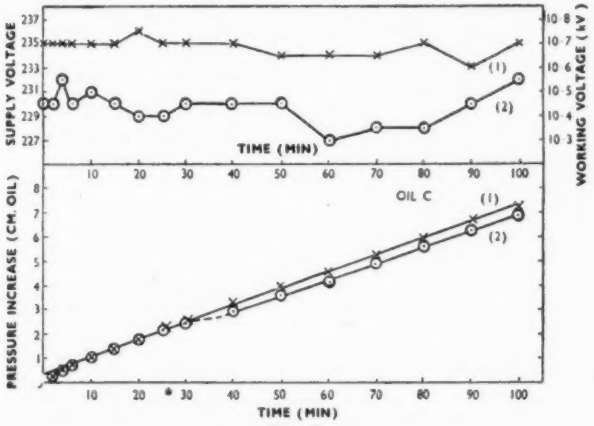

FIG. 3.

GAS EVOLUTION OF AN OIL IN THE GASSING APPARATUS.
Supply voltage variations and effect on gassing rate (original apparatus).

apparatus between experiments, and a really effective solvent for it is still lacking. It was eventually removed with the aid of a wire tipped with cotton wool. This procedure did not clean the inner electrode, which was inevitably misplaced from its axial location during the process, and could be reset only by eye. As the maximum stress in the apparatus, which occurs at the surface of the inner electrode, is critically dependent on the electrode spacing (see below), attempts were made to modify the electrode system to eliminate these cleaning difficulties. It was conjectured that the accumulation of deposit on the inner electrode and changes in its location were largely responsible for the poor long-term reproducibility of the apparatus.

Alternative Electrode Systems.

The first alternative electrode system was totally enclosed in the reaction vessel. It comprised a stainless-steel cylinder, fitting closely into the

* See Appendix II.

reaction vessel, in which a stainless-steel rod was supported co-axially by oil-resistant, insulating bushes. Spring contacts and tungsten-wire seals through the glass were used to connect the electrodes to the high-voltage supply. This electrode assembly could be removed, dismantled, cleaned, accurately reassembled, and replaced. It also had the advantage of simplifying the calculation of electric stress. It proved to be unpractical, however, owing to surface sparking across the upper bush and direct sparking between the electrodes through the gas phase. It was possible to eliminate the first effect by baking the bush at 100° C before use to remove adsorbed moisture, but the second was probably due to stress concentration at the end of the outer electrode. Its suppression by suitable alterations in the electrode assembly would have substantially increased the volume of the reaction vessel and complicated the design.

A second electrode system was devised in which the outer electrode was a heavy brass cylinder supported in the reaction vessel by a standard-taper brass-to-glass ground joint which accurately located it. The inner electrode was similarly supported and located coaxially in the outer electrode by means of a ground-glass reducing adaptor, which also served to insulate it. This electrode assembly also gave trouble due to sparking, was cumbersome, and depended on three concentric ground joints to locate and support the electrodes.

The foil electrode external to the reaction vessel was therefore retained, and the inner electrode alone modified to make it removable for cleaning and yet reproducibly located. The glass parts were also altered slightly, resulting in the modified apparatus described below.

Thornton Modified Gassing Apparatus (*Fig.* 4 *and Plate I*).

The redesigned inner electrode is a precision-ground stainless-steel rod. It is supported in the reaction vessel by a ground-glass joint (*C*) and tungsten–glass seal on the tungsten lead wire (*D*). The purpose of the small hole (*E*), in the head of the internal seal, is to facilitate the escape of any solvent vapour that may have become trapped in the head during cleaning. The glass tubing of the internal seal is selected to be a close fit to the inner electrode, and extends the entire length of the ground joint. The inner electrode is thus permanently aligned with respect to the axis of the reaction vessel. The sample is contained in a small reservoir attached to the apparatus by the ground joint (*F*). The sample inlet tube has been shifted to the top of the reaction vessel to facilitate work with high-viscosity oils, and to simplify cleaning by eliminating deposition of the solid decomposition product in the capillary, which occurred in the earlier design. The manometer (*L*) can be separated from the reaction vessel at the ground joint (*I*), and is filled with dibutyl phthalate. Stop-cocks (*K*) and (*N*) are necessary only when the apparatus is used under reduced pressure (for non-routine investigational work), and are not required for tests at atmospheric pressure. The complete assembly, including the manometer, is immersed to the level indicated in Fig. 4 in a glass tank (13 × 12 × 12 in) with flat sides, filled with a pale-coloured oil maintained at 50° ± 0·1° C, and pressure changes are measured on a mm scale. This scale is supported behind the manometer on a sheet of insulating material which also carries a split brass block which clamps

around the external foil electrode (*B*) and supports the apparatus in the thermostat. The electrodes are connected to a pair of protected terminals on the insulating sheet, from which heavily insulated leads with earthed screening sheaths go to the high-voltage supply.

The working procedure is substantially identical with that described above for the original apparatus. After each experiment the apparatus is cleaned with redistilled light petroleum spirit and dried. The inner electrode is similarly washed and then wiped with a cloth. The stopcocks and ground joints are greased, and the apparatus reassembled. The reaction vessel is cleaned more thoroughly with a test-tube brush, etc., to remove deposits after about twenty experiments.

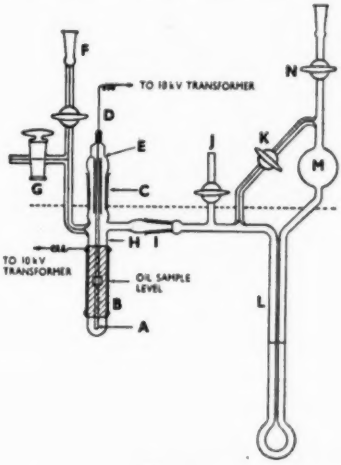

FIG. 4.

MODIFIED (THORNTON VERSION) GASSING APPARATUS.

Reproducibility of Determinations (Modified Apparatus).

In consecutive experiments on a given oil, the gassing coefficient *S* varies about the mean value by about $\pm 0{\cdot}5$ or ± 5 per cent, whichever is the greater; the units of *S* are cm dibutyl phthalate/min (multiplied by 100 as above). The long-term stability is indicated by tests on the reference oil over a period of nine months, involving a total of some 150 tests. For the reference oil, *S* varied from $+9{\cdot}0$ to $+11{\cdot}0$ or ± 10 per cent of the mean value, 10·0. During the latter 100 tests of this series, the variation in the *S* value of the reference oil was rather less, between $+10{\cdot}0$ and $+11{\cdot}0$. The performance of the apparatus is checked by frequent tests on a reference oil during the examination of groups of samples, and especially after the removal of deposit from the reaction vessel.

Study of Experimental Variables.

1. *Working voltage.* Preliminary experiments were made in the original apparatus at 50° C and hydrogen at atmospheric pressure using the oil

D and a synthetic oil (*E*), having positive and negative gassing coefficients respectively. The working voltages were obtained from taps on the high-voltage transformer secondary, and also by using a lower supply voltage on the primary. The results (Fig. 5) indicated that the rate of gas evolution or absorption increased linearly with increasing working voltage, and suggested that there was a critical minimum voltage (3 to 4 kV) below which either process would not occur.

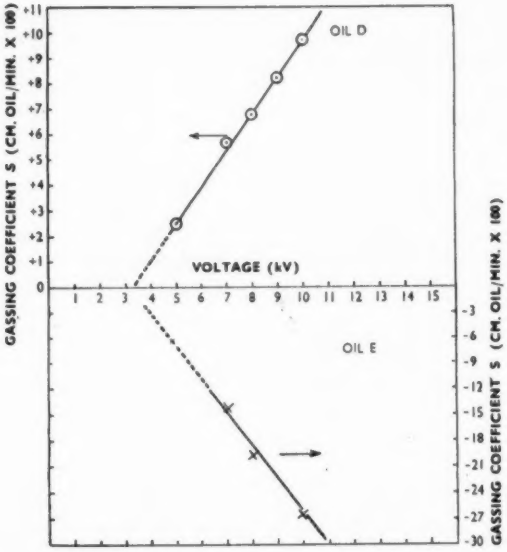

FIG. 5.

EFFECT OF WORKING VOLTAGE ON RATE OF GAS EVOLUTION AND ABSORPTION. (Original apparatus).

Further experiments were carried out in the modified apparatus on the gas-evolving oil D, using a "Variac" auto-transformer in the primary circuit to vary the voltage obtained from the secondary of the high-voltage transformer. In some tests, the applied voltage was altered several times at 1-hr intervals in the course of each experiment and the gassing coefficient, *S*, determined for each voltage. The results (Fig. 6) are anomalous; in each experiment the relation between voltage and gassing coefficient is roughly linear, but the actual gassing coefficients depend on the direction of the voltage changes. At low voltages, the corresponding gassing coefficients are highest in the experiment in which the voltage is progressively increased, and are lowest when the voltage is progressively decreased. Similarly, the gassing coefficients at the higher voltages are highest in the experiment in which the voltage is progressively decreased. The results of an experiment in which the voltage was first increased and then decreased are intermediate in character. These anomalies are possibly the result

of changes in the composition of the gas phase during the course of each experiment, resulting in a reduction of the overall rate of gas evolution owing to hydrogen absorption by unsaturated oil-decomposition products in the gas phase. This view is supported by a prolonged experiment with the same oil at a fixed voltage, in which the rate of gas evolution during the second 100-min period was less than during the first.

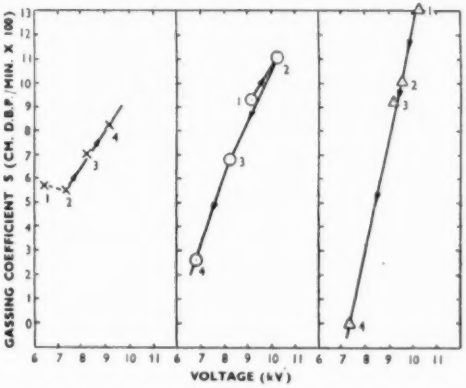

FIG. 6.

EFFECT OF WORKING VOLTAGE ON RATE OF GAS EVOLUTION.
Oil D, continuous experiments, voltage changes in orders indicated.

Separate experiments at various fixed voltages in the modified apparatus agreed with the results of the earlier tests under the same conditions in the original apparatus. The effect of using an inner electrode of smaller diameter ($\frac{1}{16}$ in) to increase the maximum value of the available range of electric stress was also studied. Under these conditions (Fig. 7), the relation between rate of gassing and applied voltage was linear up to 9·5 kV, but then appeared to remain constant with a further increase in voltage. The reason for this apparent " saturation " effect is not known. With the inner electrode of smaller diameter, agitation at the oil–hydrogen interface, which appears to be a necessary condition for the gassing process, was first observed at a lower voltage than was required with the $\frac{1}{8}$ in dia electrode, owing to the higher stress obtained at the electrode surface for the same applied voltage.

2. *Effect of temperature.* The effect of temperature on the rate of gas evolution was studied over the range 20° to 100° C with two oils (C, D) having positive gassing coefficients at the standard temperature (50° C). The results (Fig. 8) indicate that over this range the rate increases linearly with increasing temperature. If the rate of gas evolution (or absorption) was dependent solely on the vapour pressure of the oil, a relationship of a logarithmic character would be expected.

The effect of temperature on gassing rate was also determined for a high-viscosity cable oil F, but its gassing coefficient was so low ($S \simeq \pm 0{\cdot}5$) that its dependence on both temperature and voltage was within the limits

of experimental error, though the indications were that the rate of gas absorption (S negative) was lower at 70° C than at 50° C. Suitable technique and working conditions for evaluating the gassing tendencies of very high-viscosity oils have not yet been established, but useful results have been obtained for oil F (Fig. 7) and similar products in the viscosity range 400 to 900 sec (Red. I at 140° F) by working at 70° C.

Berberich [12] also found that a high-viscosity solvent-treated oil (130 sec, Saybolt Universal at 210° F, 98 V.I.) evolved gas less rapidly at 60° C than at 27° C.

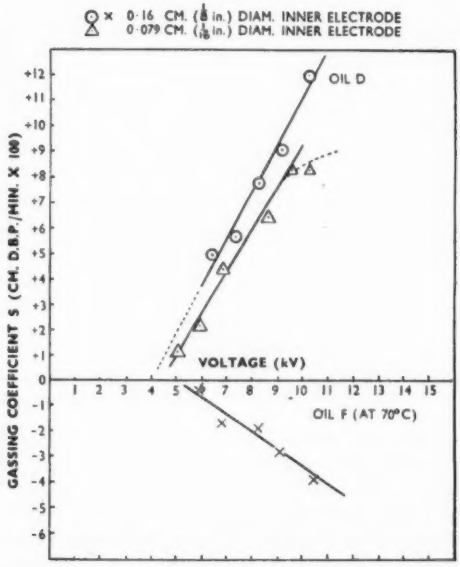

FIG. 7.

EFFECT OF WORKING VOLTAGE ON RATE OF GAS EVOLUTION AND ABSORPTION.
(Modified apparatus.)

3. *Effect of nature of gas phase.* The use of hydrogen as the gas phase in the apparatus is to some extent justified by the fact [7,10,12,16] that this gas constitutes the greater proportion (exceeding 90 per cent in many cases) of the gaseous products formed during the decomposition of hydrocarbons and petroleum oils under electric stress. Oil-impregnated paper insulation, as used in cables and capacitors, is likely to contain traces of air owing to incomplete evacuation and impregnation. The behaviour of air and nitrogen as gas phases in the apparatus was therefore studied, using three oils (D, G, H) with widely different gassing characteristics when evaluated under hydrogen.

Under nitrogen at atmospheric pressure, all three oils *evolved* gas. The plots of pressure increase *vs* time were not linear (Fig. 9), but the final slopes were of the same order for the two oils which had positive S values

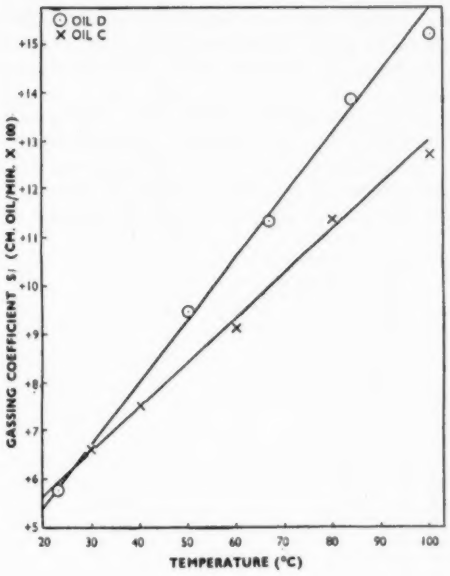

FIG. 8.

VARIATION OF GAS EVOLUTION RATE WITH TEMPERATURE.

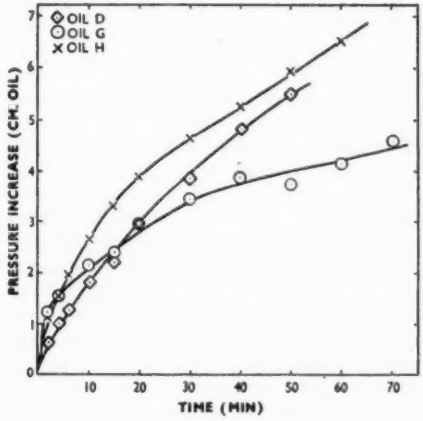

FIG. 9.

GAS EVOLUTION UNDER NITROGEN.

under the normal conditions. The final slope of the curve for the normally absorbing oil was rather lower, corresponding to an S value of *ca* +4·5. The final gassing rates under nitrogen were slightly lower than the values obtained under hydrogen in the case of the two oils with positive normal S values.

The observed gassing behaviour of an oil in the gassing apparatus is presumably determined by the relative contributions of the various constituents to hydrogen-evolving or absorbing processes, depending on their chemical structure. For a gas-evolving oil the overall rate of gas evolution exceeds the rate of absorption, and conversely in the case of an

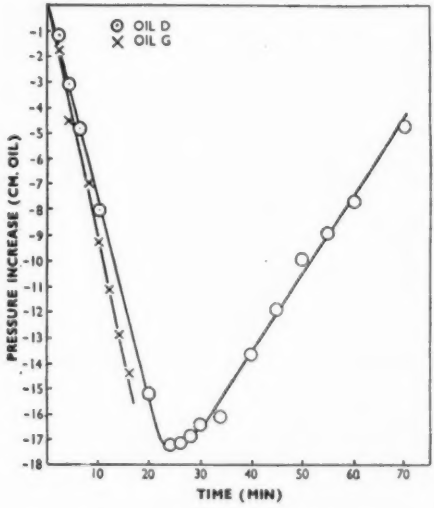

FIG. 10.

GASSING CHARACTERISTICS OF OILS UNDER AIR.

absorbing oil. It would be expected that under nitrogen, the hydrogen-absorbing processes would be absent so that the gas-evolving constituents alone would determine the net gassing characteristics. The results obtained under nitrogen are in agreement with these views.

Oils D and G, with positive and negative gassing coefficients respectively under the standard conditions, were also examined under air at atmospheric pressure (Fig. 10). In both cases absorption occurred at a uniform rate for a period of 15 to 20 min. In the experiment with oil D for which the stress was maintained beyond this period, the absorption process was followed by gas evolution again at a uniform rate, with the plot of pressure *vs* time passing through a well-defined minimum at *ca* 25 min. The slope of the second part of the plot for oil D corresponded to a gassing coefficient of *ca* +31, which is much higher than the value for the same oil under hydrogen. These results are explicable on the view that for both oils the initial process is the absorption of the oxygen in the gas phase, followed by

gas evolution in the residual atmosphere of nitrogen. It may be noted that the total volume of gas absorbed by oil D in the experiment under air at atmospheric pressure is of the order of 2 ml for a manometer with an internal diameter of 2 mm and a decrease in pressure of 17 cm of oil (Fig. 10). Since the total volume of air initially confined between the surface of the sample and the manometer is (very roughly) *ca* 10 ml, the volume contraction during the absorption is approximately equal to the total volume of oxygen initially present in the gas phase. In discussing chemical reaction induced by ions formed by high-energy α-particles from radon, Lind and Bardwell [15] have pointed out that the high affinity of oxygen for free electrons produces an important effect, by which oxidation replaces the other reactions that would occur in its absence.

4. *Influence of position of oil–gas interface relative to electrodes, and behaviour of the oil–gas interface.* Several experiments were carried out in the original apparatus with oil D, having a positive gassing coefficient under the standard conditions, in which the position of the oil–gas interface relative to the electrodes was altered from the location indicated in Fig. 1. When the oil level was raised above the inner electrode, which was then completely submerged, no gas evolution occurred. A similar result was obtained by lowering the oil surface below the level of the bottom of the outer electrode. In both cases the characteristic disturbance of the gas–oil interface which accompanies gas evolution or absorption was also absent. Experiments in which the volume of the gas phase under stress was varied by altering the level of the oil–gas interface, within the limits of the outer electrode, indicated that the overall rate of gas evolution for a given oil increased with increasing volume of stressed gas phase. Under the standard conditions, this factor is maintained constant by working at a fixed oil level indicated by the mark (*a*) in Fig. 1.

As the voltage applied to the electrodes was increased from zero, no disturbance of the oil–gas interface was apparent up to a value of *ca* 5 kV, when slight intermittent oscillations of the oil surface occurred. Observations made in the dark showed that this point coincided with the appearance of corona on the part of the inner electrode exposed to the gas phase. As the voltage was increased up to the maximum available value of 10 kV, both the disturbance of the interface and the intensity of the corona discharge became more pronounced. The results shown in Fig. 5 suggest that the minimum voltage required to obtain gas evolution or absorption is of the order of 3 to 4 kV.

At 10 kV other effects were visible at the oil–gas interface. Humping of the oil, to a height of several millimetres, occurs around the inner electrode. This behaviour is probably an example of the electrostatic phenomenon known as dielectric displacement; [25] a dielectric in a non-uniform field tends to move to the region of highest electric stress, in this case the surface of the inner electrode.

The stress distribution causing this effect arises from an alternating voltage, and the entire surface of the oil becomes violently agitated, since the result of the successive displacements is presumably to impart an oscillatory movement to the oil at the interface. This effect, together with the deposition of oil droplets on the wall of the reaction vessel above the interface, probably serves to increase the overall rate of gas evolution

or absorption by facilitating interaction between the oil and the high-energy ions and electrons generated by the corona discharge in the gas phase. In this connexion, it was noted in experiments with high-viscosity oils that solid products were deposited on the wall of the reaction vessel *above* the interface, in addition to that normally found below the interface with low-viscosity oils. This behaviour is consistent with the view that droplets of high-viscosity oil on the wall of the reaction vessel return less rapidly to the oil surface, and are therefore exposed to ionic bombardment

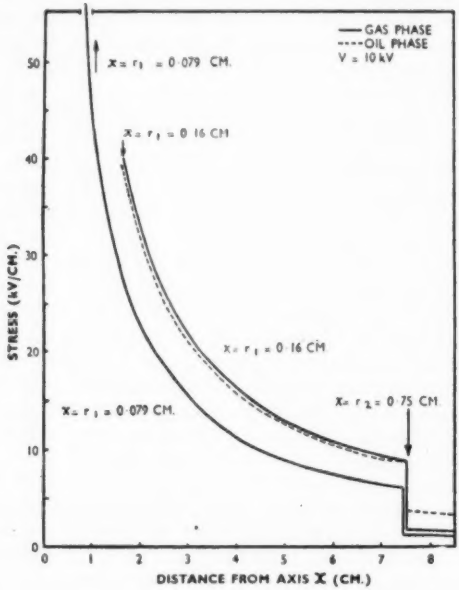

FIG. 11.

RADIAL VARIATION OF ELECTRIC STRESS IN GASSING APPARATUS.

for longer periods than droplets of low-viscosity oils, sufficiently so to deposit solid decomposition products in this region. With low-viscosity oils, the high degree of turbulence at the oil–gas interface also produces a fine spray of oil droplets which deposits oil on the wall of the reaction vessel extending well above the region of the electrodes. The distribution of oil into the gas phase also influences the corona discharge at the inner electrode; the voltage at which the discharge ceased as the voltage was progressively decreased was slightly lower than the voltage at which it started as the voltage was raised, owing presumably to the oil film on the inner electrode which lowers the corona threshold.*

Foaming at an oil–gas interface under electric stress has been described by Becker [19] and Evers; [20] their observations indicate that the final state

* See Appendix I.

is preceded at lower voltages by a reversal in form of the oil meniscus and the appearance of gas bubbles.

Magnitude of Electric Stress in the Gassing Apparatus.

Application of electrostatic theory for a capacitor of the coaxial cylindrical type to the electrode of the gassing apparatus shows (Fig. 11) that the maximum stress occurs at the surface of the inner electrode and decreases radially, according to an inverse logarithmic function of the ratio of the electrode radii. The stress falls abruptly at the wall of the reaction vessel owing to the change in permittivity (dielectric constant). The maximum stresses and their radial variations are nearly equal in the gas and oil phases, but the change at the wall of the reaction vessel is greatest for the gas phase, where the change in permittivity is greatest.

For the B.P.M. version of the apparatus with the dimensions of Fig. 1, the maximum stress for 10 kV applied voltage is 47·8 kV/cm and 71·7 kV/cm for 15 kV. For the Thornton version (Fig. 4), the values are 40 and 60 kV/cm respectively. Reducing the diameter of the inner electrode from $\frac{1}{8}$ to $\frac{1}{16}$ in increases the maximum stress for 10 kV from 40 to 55·5 kV/cm. All these values refer to the gas phase. The equations used to calculate the stress are given in Appendix I.

For hydrogen, nitrogen, and air at atmospheric pressure and 50° C, the minimum stresses required to cause corona discharge at the surface of the inner electrode (0·16 cm, $\frac{1}{8}$ in dia) are all lower than the maximum stress (40 kV/cm) attained with an applied voltage of 10 kV.

Discussion.

During the past four years the gassing apparatus has been used in this laboratory, in both its original and modified forms, for the routine evaluation of the relative gassing tendencies of insulating oils, and also for studying, in some detail, the relation between gassing tendency and chemical composition of a wide range of petroleum oils and related hydrocarbon products. For both these applications the increased reproducibility obtained in duplicate tests, and the long-term reproducibility, as shown by check tests over long periods with reference oils, have justified the introduction of the modifications described in this report, despite the increased design complexity. For both types of work it has proved adequate to express the relative gassing tendencies of oils numerically by the gassing coefficient, S, described previously. The standard working conditions for samples in the transformer oil viscosity range are :—

Temperature	$50 \pm 0{\cdot}1°$ C
Gas phase	Hydrogen at atmospheric pressure
Applied voltage	10 kV (r.m.s.)
Max stress at surface of inner electrode (calc)	40 kV/cm (r.m.s.)

The last figure applies to an apparatus with the electrode size and spacings, etc., shown in Fig. 4. For high-viscosity products of the cable-oil type the temperature has been raised to 70° C in the few experiments so far carried out.

Before commenting on the significance of the relative gassing coefficients obtained by this method, it may be stated that the results obtained on oils of widely different hydrocarbon-type composition are in general agreement with the findings of previous workers regarding the influence of this factor, and therefore of feedstock type and refining treatment, on the tendency of insulating oils to decompose under electric stress. This aspect of the subject will not be discussed further here, but it should be emphasized that the gassing test does enable simple and very valuable quantitative correlations to be set up between the gassing coefficients and various analytical characteristics of insulating oils, irrespective of its possible inadequacy in simulating service conditions in cables and capacitors.

The first point for criticism is the magnitude of the maximum stress used. A value of 40 kV/cm corresponds to *ca* 100 V/mil (1 mil = 0·001 in) which may be compared with stresses of the order 300 to 400 V/mil in capacitors *

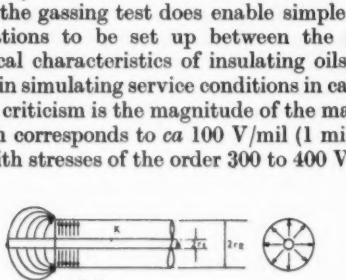

FIG. 12.

LINES OF ELECTRIC FORCE IN GASSING APPARATUS AND DISPOSITION OF DIELECTRICS.

and 100 to 250 V/mil in cables encountered under commercial service conditions. The maximum stress obtained in an apparatus of the dimensions used here just approaches the value (100 V/mil) encountered in 33-kV solid-type cable, but does not attain the higher stresses found in gas-compression cables and capacitors, even if the applied voltage is increased to, say, 15 kV, as is sometimes done.

It is probable that the surface of the inner electrode is not the only region of high stress in the apparatus. The differences in length of the inner and outer electrodes must result in a high density of lines of electric force, where these converge at the ends of the outer electrode (Fig. 12). Since one of these regions of high flux density is in the gas phase, it may influence the gassing process. No attempt has been made to assist the stress in this region, but it is interesting to note that no punctures of the glass wall of the reaction vessel in this region have been observed. On the other hand, however, the surface sparking across insulating end bushes in the trials of alternative electrode systems may be recalled.

It is evident from the results shown in Fig. 9 for oil D that the behaviour

* For A.C. service; may be 1000 to 1300 V/mil on D.C.

of this *gas-evolving* oil is qualitatively similar under hydrogen and nitrogen. Oxygen is clearly undesirable as the gas phase for routine tests, in view of Lind and Bardwell's evidence that reactions between hydrocarbons and the O_2-ion, etc., probably occur at the expense of other reactions of the hydrocarbons alone. The relatively high reactivity of oxygen is of practical importance, however, as this gas will constitute part of any traces of air remaining in vacuum-impregnated paper insulation, or may be produced by the decomposition under electric stress of water formed by thermal decomposition of the paper. Absorption of oxygen from air at reduced pressure in artificial voids in oil-impregnated paper has been observed by Sommerman.[13] The influence of electric stress on the reaction between oil and oxygen in the liquid phase was considered in the A.S.E.A.–Anderson [21] oxidation test for transformer oils, but its relevance has been criticised.[22]

The use of hydrogen as the gas phase has the advantage of increasing the discrimination of the test by distinguishing between oils which *evolve* and those which *absorb* hydrogen under electric stress. Since relative absorbing tendencies can also be correlated with oil composition this distinction is of great value, but is not obtained with nitrogen as the gas phase (Fig. 9, oil H) or by working under vacuum.[12] The ability to assess hydrogen-absorbing properties is also of practical importance in view of the possible use of additives [11, 12] to convert gas-evolving into gas-absorbing oils, and of synthetic hydrocarbon products [23] with extremely marked hydrogen-absorbing tendencies.

It has frequently been assumed in earlier work on liquid hydrocarbons and oils that the effects observed under electric stress are essentially gas-phase phenomena. It has similarly been assumed that the formation of solid decomposition products of the insulating oils in cables and capacitors requires the presence in the insulation of voids containing air in which discharges may be initiated. The results of Nederbragt [11] on the effect of relatively volatile materials on the gas evolution of insulating oils are in agreement with this view, which is also supported by the work described in this report on the influences of temperature and position of the oil–gas interface. As pointed out above, however, the linear relation between temperature and rate of gas evolution is not entirely consistent with the simple picture of oil vapour as the material undergoing decomposition. The foaming observed at the oil–gas interface and the resulting production of oil spray from low-viscosity products suggests a mechanism by which small oil droplets may be bombarded with gaseous ions produced by the discharge in the gas phase. Such a picture is similar to that proposed for the void discharges in impregnated paper, for which it has been suggested that gaseous ions are accelerated by the electric field acting across the void, and are stopped at the void boundary by collision with oil films. In the light of the available evidence, it seems reasonable to ascribe the decomposition of hydrocarbon oils under electric stress, both in the apparatus described, and in oil-impregnated paper insulation, to a combination of both these processes, viz., a true vapour-phase interaction between oil molecules and gaseous ions, and the bombardment of oil droplets or surfaces.

The possibility that decomposition may also occur as a true liquid-

phase process in bulk oil cannot be overlooked, but the available information on true liquid-phase corona is scanty. For insulating oils, the work of Peek [24] suggests that corona and break-down (spark-over) may be practically coincident.

On the basis of the various considerations outlined above, it is suggested that the results obtained in the gassing apparatus have some relevance to the behaviour of insulating oils under the conditions existing in oil-impregnated paper insulation. It is clear, however, that a fundamental investigation of the gassing process would entail a study of, *inter alia*, the following points :—

(*a*) use of higher stresses, equal to or greater than those involved in practice;

(*b*) a differentiation between the separate gas-phase and liquid-phase processes;

(*c*) the behaviour of hydrogen, oxygen, nitrogen, and volatile oil additives over a wide range of pressures;

(*d*) a study of the gassing process in *oil-impregnated paper*, preferably in conjunction with suitable equipment to detect the occurrence of internal discharges in such insulation.

Until further information on these points is available, the gassing apparatus with the modifications described, and used under standardized test conditions, may be regarded as a useful tool for the routine evaluation of relative gassing tendencies.

Conclusions.

1. The modified apparatus and recommended working procedure have improved the long-term reproducibility of the gassing test, which is of the order of $\pm 0{\cdot}5$ on the gassing coefficient or ± 5 per cent (whichever is the greater).

2. Under the standard test conditions the gas evolution or absorption rate of an oil increases linearly with increasing voltage above a certain value of the latter, below which no evolution or absorption occurs.

3. For a gas-evolving oil, the rate increases linearly with temperature over the range 30° to 100° C.

4. Independently of their behaviour under hydrogen, the oils examined evolve gas under nitrogen. When the gas phase is air, the evolution process is proceded by an initial period of absorption.

5. The gassing process appears to be mainly located at the oil–gas interface, and if this is not situated in a region of electric stress, the gassing phenomena are suppressed. The process is associated with visible turbulence of the interface.

6. The present apparatus is not suitable for a fundamental study of the gassing process, although it is satisfactory for evaluating the relative gassing tendencies of insulating oils. Alternative experimental methods for the investigation of the phenomena are briefly indicated.

Acknowledgments.

The authors are indebted to H. C. Evans and D. V. Tilston (deceased), who carried out the initial investigations, to J. A. H. Counsell for his

calculations of the stresses involved, and also to B. H. Moerbeek (Amsterdam laboratory of the N.V. de Bataafsche Petroleum Maatschappij) and his colleagues. Thanks are also due to "Shell" Refining and Marketing Co., Ltd., for permission to publish this paper.

THORNTON RESEARCH CENTRE,
THORNTON-LE-MOORS,
CHESTER, ENGLAND.

APPENDIX I.

CALCULATION OF STRESS IN THE GASSING APPARATUS.[24]

For a simple co-axial electrode system the radial variation of stress is given by :—

$$G_x = \frac{V}{x \,.\, \ln r_3/r_1} \quad . \quad . \quad . \quad . \quad . \quad . \quad . \quad . \quad . \quad (1)$$

where G_x = stress (V/cm) at a distance x cm from the axis of the electrodes,
V = applied voltage,
r_1 = radius of inner electrode in cm,
r_3 = radius of outer electrode in cm.

This equation does not involve the permittivity, K, of the medium. The apparatus may be regarded (Fig. 12) as two capacitances in parallel, each involving two dielectrics in series. Neglecting end effects, the lines of electric force are radially symmetrical and normal to the axis of the electrodes. Equation (1) is replaced by :—

$$G_x = \frac{1}{x \,.\, K_x} \cdot \frac{V}{\dfrac{\ln r_3/r_1}{K_1} + \dfrac{\ln r_3/r_2}{K_2}} \quad . \quad . \quad . \quad . \quad . \quad . \quad . \quad (2)$$

Where K_x = Permittivity of the dielectric at radius x,
K_1 = Permittivity of dielectric No. 1,
K_2 = Permittivity of dielectric No. 2,
r_1 = Radius of inner electrode,
r_2 = Internal radius of outer electrode,
r_3 = External radius of outer electrode.

For the apparatus of Figs. 1 and 4.

K_1 = 1 (hydrogen),
= 2·2 (oil at 50° C, average value),
K_2 = 5 (Pyrex glass),
r_1 = 0·125 cm (B.P.M. apparatus); 0·16 or 0·079 cm (T.R.C. apparatus),
r_2 = 0·65 cm (B.P.M. apparatus); 0·75 cm (T.R.C. apparatus),
r_3 = 0·75 cm (B.P.M. apparatus); 0·85 cm (T.R.C. apparatus).

These values were used to construct Fig. 11 and calculate the figures for G_x given above.

MINIMUM STRESS FOR CORONA DISCHARGE.

For concentric cylindrical electrodes with air as dielectric :—

$$G_v = 31\,\delta\,(1 + 0{\cdot}308/\sqrt{\delta r}) \text{ max kV/cm}$$

where G_v = Minimum gradient at surface of inner electrode for visible corona,
δ = Air density (unity at pressure of 76 cm mercury and 25° C; $\delta = 3{\cdot}92\,p/273 + t$),
r = Radius of inner electrode in cm.

For air at 50° C and 76 cm pressure, δ = 0·92 and for r = 0·16 cm, G_v = 51·5 max kV/cm or 36·4 r.m.s. kV/cm. G_v is lowered slightly by a film of oil on the electrode, and the appropriate formula gives G_v = 35·4 r.m.s. kV/cm. The critical corona stresses for oxygen and hydrogen are slightly and markedly lower respectively than for air. The values for air and nitrogen are practically identical.

APPENDIX II.

Key to Oil Samples Code.

A. White oil: viscosity 45 sec Redwood I at 140° F, 115 to 135 sec Redwood I at 70° F.
B. Crude distillate: viscosity 100 sec Redwood I at 140° F.
C. White oil: viscosity Saybolt Universal 80 to 90 sec at 100° F.
D. Transformer oil: B.30 class (B.S. No. 148, 1933).
E. Synthetic oil: viscosity 54 sec Redwood I at 140° F.
F. Cable oil: viscosity 389 sec Redwood I at 140° F.
G. Crude distillate: viscosity 45 sec Redwood I at 140° F.
H. Solvent-refined, acid-treated oil: viscosity 45 sec Redwood I at 140° F.

References.

[1] Lind, S. C., Bardwell, D. C., and Perry J. H. *J. Amer. chem. Soc.*, 1926, **48**, 1556.
[2] Lind, S. C., and Bardwell, D. C. *J. Amer. chem. Soc.*, 1926, **48**, 2335.
[3] Lind, S. C., and Glockler, G. *J. Amer. chem Soc.*, 1928, **50**, 1767.
[4] Lind, S. C., and Glockler, G. *J. Amer. chem. Soc.*, 1929, **51**, 2811.
[5] Lind, S. C., and Glockler, G. *J. Amer. chem. Soc.*, 1929, **51**, 3655.
[6] Lind, S. C., and Glockler, G. *J. Amer. chem. Soc.*, 1930, **52**, 4450.
[7] Schoepfle, C. S., and Fellows, C. H. *Industr. Engng Chem.*, 1931, **23**, 1396.
[8] Linder, E. G., and Davis, A. P. *J. phys. Chem.*, 1931, **35**, 3649.
[9] Honig, R. E., and Sheppard, C. W. *J. phys. Chem.*, 1946, **50**, 119, 144.
[10] Schoepfle, C. S., and Connell, L. H. *Industr. Engng Chem.*, 1929, **21**, 529.
[11] Nederbragt, G. W. *J. Inst. elec. Engrs*, 1936, **79**, 282.
[12] Berberich, L. J. *Industr. Engng Chem.*, 1938, **30**, 280.
[13] Sommerman, G. M. L. *Elect. Eng.*, 1937, **56**, 566.
[14] Moerbeek, B. H. Private Communication.
[15] Lind, S. C., and Bardwell, D. C. *J. Amer. chem. Soc.*, 1925, **47**, 2675.
[16] Sticher, J., and Thomas, D. E. F. *Trans. Amer. Inst. elect. Engrs*, 1939, **58**, 709.
[17] Thompson, A. W., and Wood-Mallock, J. C. *J. Inst. elec. Engrs*, 1943, **90**, 35.
[18] Meyer, F. *J. Inst. elec. Engrs*, 1940, **86**, 313.
[19] Becker, H. *Wissenschaftliche Veröffentlichungen aus dem Siemens-Konzern*, VIII (2), 199.
[20] Evers, F. *Siemens Zeitschrift*, April 1935, 125.
[21] Anderson, B. *A.S.E.A.J.*, 1935, pp. 83, 99, 118.
[22] Pollitt, A. A. *J. Inst. Petrol.*, 1946, **32**, 420.
[23] B.P. 557,321 (accepted Nov. 16, 1943) to Shell Development Co.
[24] Peek, F. W. "Dielectric Phenomena in High-Voltage Engineering" (McGraw-Hill, New York, 3rd. Edn. 1929).
[25] Gemant, A. "Liquid Dielectrics" (Wiley, New York, 1933); pp. 104–111.

"KNOCK" TESTS USING AN ATMOSPHERE IN WHICH NITROGEN IS REPLACED BY ARGON AND CARBON DIOXIDE.

By D. Downs * (Associate Fellow) and J. H. Pignéguy.*

Introduction.

It has been well established that during combustion in a petrol engine, oxides of nitrogen are formed, varying in quantity with the chemical composition of the fuel and produced in greater amount under "knocking" conditions. The concentration of nitrogen peroxide in gases sampled from the combustion chamber during the cycle has been shown [1] to increase throughout the latter part of the compression and the early part of the expansion strokes. In some cases oxides of nitrogen have been shown to be present before the passage of the spark. It has not been demonstrated with certainty, however, that the nitrogen compounds are present in the cylinder as NO_2, and it seems more likely that they are there as NO, which is oxidized to NO_2 in the passage from the sampling valve to the analyzer.

Many theories have been put forward to account for the formation of nitrogen compounds and to explain their effect on "knock" in the engine. The general conclusion seems to be that nitrogen itself is not among the actual causes of "knock," but that the same conditions which encouraged this phenomenon also encourage the formation of nitrogen compounds, *e.g.*, the higher exhaust-valve temperature when "knocking" might, by catalytic action on its surface, increase the nitrogen oxide concentration.

The fact that with the higher paraffinic fuels at any rate, the introduction of nitrogen peroxide into the engine via the intake air stream had only a very slight effect on "knock," while the pro-knock effect of organic peroxides was considerable,[2] gave support to the theory that nitrogen peroxide was an accompaniment to "knock" rather than its cause.

The tests now described were carried out in order to determine the effect on "knock" of eliminating nitrogen from the atmosphere burning in the engine and substituting in its place: (1) an inert gas, argon; and (2) a mixture of argon and carbon dioxide thermodynamically equivalent to normal air. In this way it was hoped that a true assessment could be made of the part played by nitrogen compounds in the "knocking" process.

Description of the Apparatus.

Engine. The engine used for the tests was a Ricardo E6 type variable-compression fuel-research engine (Figs. 1 and 2). This unit has a bore of 3 in and a stroke of $4\frac{3}{8}$ in, giving a capacity of 507 cc. The compression ratio can be varied between 4·5 and 20 while the engine is in operation.

---

* Fuel Research Engineer, Ricardo & Co. Engineers (1927) Ltd.

Test Equipment. The engine is fitted with a fuel system (Fig. 3) designed to eliminate slight changes in fuel flow which, in the case of a normal carburettor, may be caused by small variations in fuel head over short periods and by the effect of vibration on fuel flow through the metering orifice.

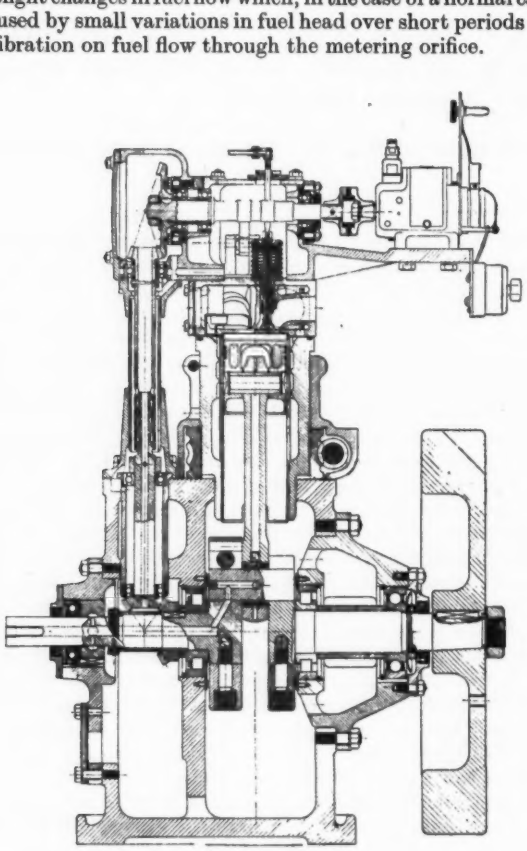

FIG. 1.

RICARDO E6 VARIABLE-COMPRESSION ENGINE—LONGITUDINAL SECTION.

The fuel is introduced into the induction pipe through an orifice under a controlled pressure. The orifice (0·010 to 0·012 in diameter) is located in a bend in the pipe with the jet impinging on a gauze pack below. The fuel is fed to the orifice through a flexible pipe attached to a heavy weight suspended by a rope—a device designed to eliminate vibration in the fuel line. Compressed air is in communication with the fuel through a fixed orifice from a constant-pressure air line, and the pressure on the line is hand-controlled by a bypass bleed to atmosphere. This pressure, in turn, controls the delivery of fuel to the engine.

For the tests on special gas mixtures, a modified induction system, as

shown in Fig. 4, was used. The engine was supplied by two separate gas lines, each provided with an Alcock viscous flow meter (*W* and *M*) and with a control valve (*B* and *P*) for adjusting the flow to give the desired proportion of each gas. A pulsation damping diaphragm (*N*) was also fitted to eliminate resonance effects in the pipework.

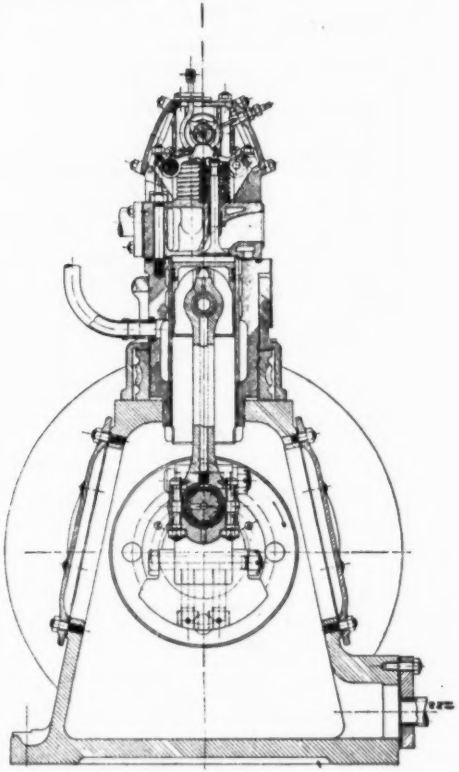

FIG. 2.

RICARDO E6 VARIABLE-COMPRESSION ENGINE—TRANSVERSE SECTION.

The cylinders containing the special gases were connected through release valves to a common capacity on the supply side of the main gas-control cock (*P*). Six gas cylinders could be connected at one time permitting a maximum running time at 1500 r.p.m., operating solely on cylinder gas, of about 30 minutes. A manometer was connected to the induction pipe close to the inlet port so that a constant air-inlet pressure could be maintained for comparative tests.

The viscous flow meter was calibrated against a standard orifice on air. A viscosity correction was applied to the meter readings when other atmospheres were being measured.

The gases used in the tests, argon and carbon dioxide, were obtained from the British Oxygen Co. as pre-mixed "airs." The argon "air" contained 77 per cent vol argon, 2 per cent vol nitrogen, 21 per cent vol oxygen and the carbon dioxide "air" contained 79 per cent vol carbon dioxide, 21 per

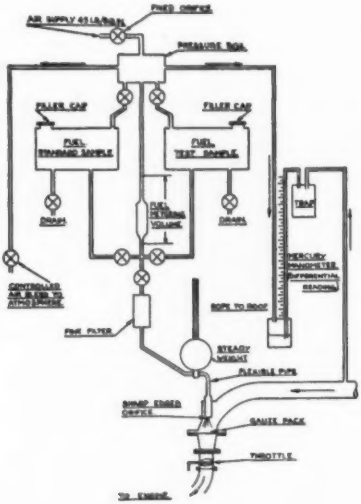

FIG. 3.

DIAGRAM OF FUEL SYSTEM.

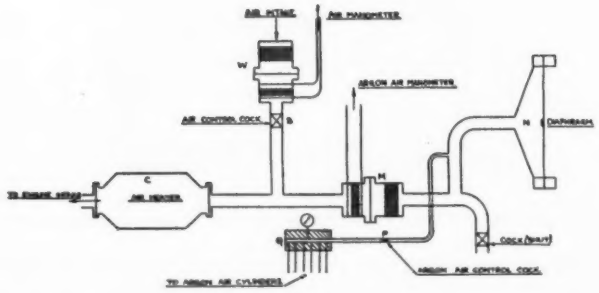

FIG. 4.

DIAGRAM OF AIR AND GAS METERING SYSTEM.

cent vol oxygen. In addition to these a "match air," consisting of a mixture of argon and carbon dioxide "airs" thermodynamically equivalent to normal air, was also obtained. The method used to determine the "match" is described in a later section.

The compositions of the fuels used in the tests are given in Table I.

TABLE I.

Properties of Fuels Used in the Tests.

1. *Standard No.* 2. Sp. gr., 0·687 at 15° C.

Composition :	Per cent by vol.
*neo*Hexane	25
Alkylates	55
*iso*Pentane–alkylates	20
Octane number (CFR/MM) 91	

2. *B.A.M.* 100. Air Ministry 100-octane reference fuel. Sp. gr., 0·710 at 15° C.

Composition :	Per cent.
Hydrobase	43
Hydrocodimer	40
*iso*Pentane	14
Aromatics	3
T.E.L.-4 ml/I.G.	—

3. *Technical* isooctane. Sp. gr., 0·703 at 15° C.

TEST PROCEDURE.

The "knock" ratings were carried out using the audibility method. When running on a particular fuel and "air," the compression ratio was

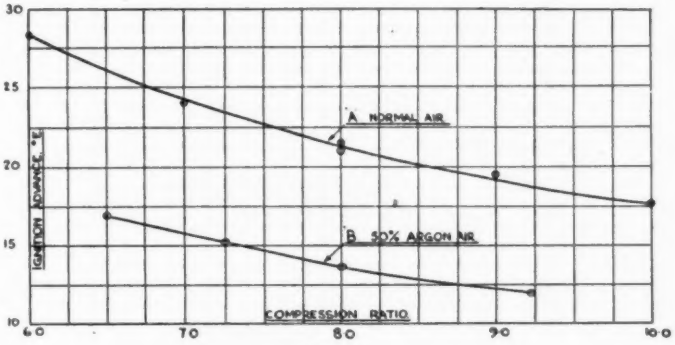

FIG. 5.

OPTIMUM IGNITION ADVANCE OVER COMPRESSION RATIO RANGE.

Maximum power mixture strength. Fuel—100 octane petrol.

raised until a standard intensity of detonation called FS/OMD (frequent slight/occasional moderate detonation) as judged by ear was reached. This limiting compression ratio, termed the H.U.C.R. (highest useful compression ratio) was taken as a measure of the knocking tendency of the fuel. Unless otherwise stated, the mixture strength used was that giving maximum knock. This was obtained either by determining the knock-limited compression ratio at a series of mixture strengths and obtaining the minimum from the resultant curve of knock-limited C. R.v mixture strength or, by setting the mixture strength and compression ratio directly to the H.U.C.R. at maximum knock mixture strength, a direct adjustment relatively easy to make with experience.

The ignition timing used was the optimum for maximum power mixture strength at each compression ratio. This timing decreases with increase in compression ratio as shown in Fig. 5.

The following engine conditions were maintained constant throughout the whole series of tests :—

Engine speed, 1500 r.p.m.
Inlet manifold depression, $\frac{1}{2}$in Hg.
Inlet air temperature, 30° C.
Jacket coolant temperature, 70° C.

"KNOCK" TESTS WITH ARGON "AIR" MIXTURES.

1. *Tests with Unleaded Fuel.*

For the first test a typical unleaded isoparaffinic fuel (Standard No. 2) was used, and the effect on its knock-limited compression ratio of replacing

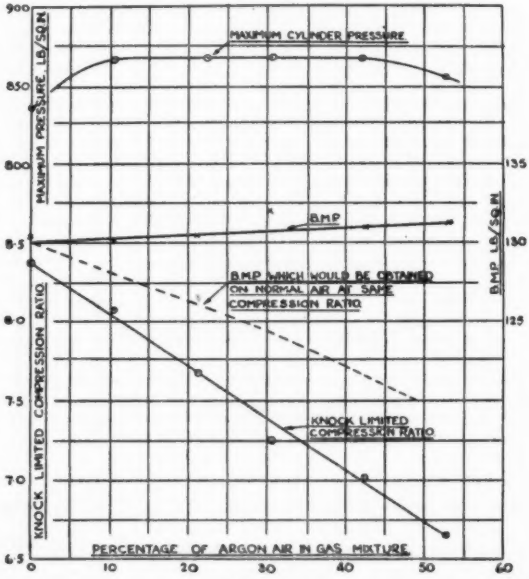

FIG. 6.

EFFECT ON KNOCK-LIMITED COMPRESSION RATIO OF STANDARD NO. 2 PETROL OF REPLACEMENT OF NITROGEN BY ARGON.

Maximum knock mixture strength (for normal air). 1.A. optimum for maximum power mixture on normal air.

the nitrogen in the air by argon was determined. To enable the tests to be carried out rapidly, the mixture was not set to give maximum knock on each "air," but the maximum knock fuel flow determined for normal air was used with all gas mixtures. Subsequent tests showed that the addition of

argon did not appreciably affect the maximum knock fuel flow, and so no error was incurred in making this assumption. The ignition advance used was the optimum for maximum power mixture on normal air (curve "A" of Fig. 5).

The results are summarized in Fig. 6, from which it can be seen that the knock-limited compression ratio falls in an approximately linear manner

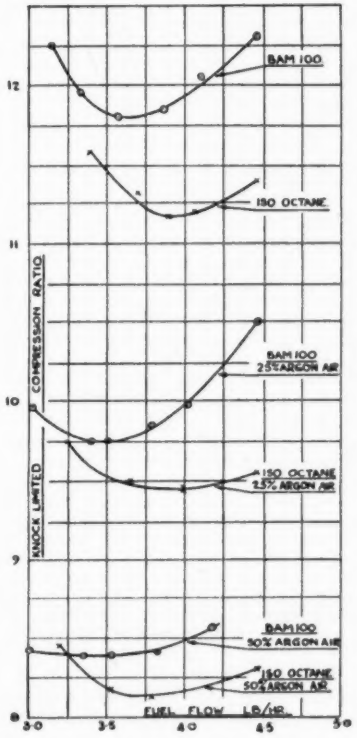

FIG. 7.

H.U.C.R.—MIXTURE STRENGTH CURVES ON ISO-OCTANE AND B.A.M. 100 USING NORMAL AIR, 25 PER CENT ARGON "AIR," AND 50 PER CENT ARGON "AIR."

I.A.—as in Fig. 5.

with increasing argon "air" content. The B.M.P., however, rises slightly with addition of argon "air," instead of falling steadily with the compression ratio as would have occurred with normal air. For a 50 per cent argon "air" mixture, the rise of B.M.P. compared with what would be obtained with normal air is 11 p.s.i.

These results demonstrate that knock-limited C.R. is not always a reliable guide to the knocking tendency of a fuel or engine in cases where the atmosphere is being varied and where in consequence the more funda-

mental quantities of knock-limited "end-gas" pressure and temperature do not bear a direct relationship to the compression ratio. In the case of these tests it is obvious that the much smaller specific heat of argon as compared with nitrogen is giving relatively higher "end gas" pressures and temperatures for a given compression ratio and that this effect is entirely masking the effect of the replacement of nitrogen by argon on the H.U.C.R.

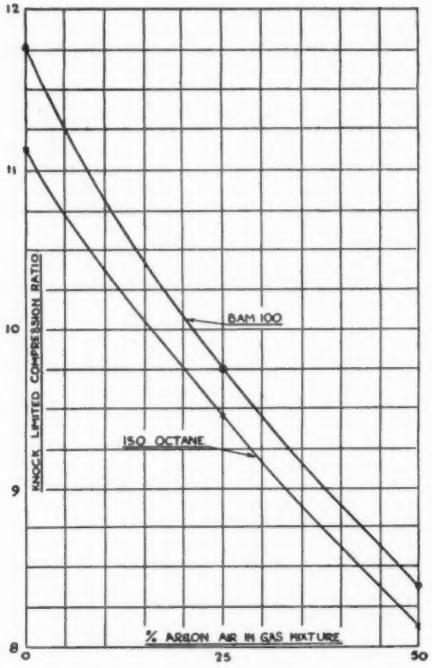

FIG. 8.

EFFECT ON KNOCK-LIMITED COMPRESSION RATIO OF (*a*) ISO-OCTANE, and (*b*) B.A.M. 100 OF REPLACEMENT OF NITROGEN BY ARGON.

Maximum knock mixture strength. 1.A—as in Fig. 5.

of Standard No. 2 fuel. The measured maximum pressures at the H.U.C.R.s, which are in effect knock-limited "end gas" pressures (Fig. 6), remain sensibly constant on addition of argon, and this suggests that, despite the big change in C.R., very little change has actually occurred in the pressure and temperature conditions at the H.U.C.R.

2. *Tests with Leaded Fuels.*

Some tests were next carried out on leaded fuels with various proportions of argon "air" in order to investigate the effect of the replacement of nitrogen by argon on the lead response of a fuel.

Full H.U.C.R. *v* mixture strength curves were obtained both on *iso*octane

and on Air Ministry 100-octane reference fuel, the latter containing 4 cc T.E.L/I.G. (Fig. 7). For the tests with normal air and with 50 per cent argon "air" the appropriate optimum ignition advance, taken from the curves of Fig. 5, were used. For the tests with 25 per cent argon "air," the mean of the optimum advances for normal air and for 50 per cent argon "air" was used. The results are summarized in Fig. 8.

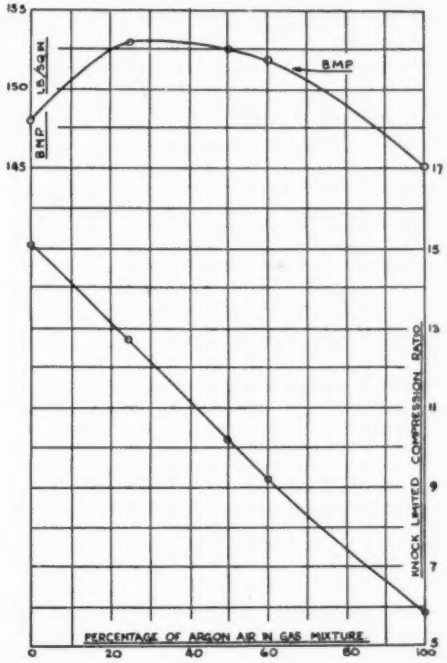

FIG. 9.

EFFECT ON KNOCK-LIMITED COMPRESSION RATIO OF ISO-OCTANE + 4 C.C. TEL/I.G. OF REPLACEMENT OF NITROGEN BY ARGON.

Maximum knock mixture strength. I.A. optimum for maximum power mixture strength in each air.

The reduction in H.U.C.R. for a given percentage of argon "air" appears to be much the same for both the leaded and the unleaded fuels. The maximum knock-mixture strength moves slightly weaker with increasing proportions of argon "air," both with the leaded and with the unleaded fuels. The differences are, however, slight.

In this experiment, the different nature of the base fuels introduced an additional complication into the comparison between a leaded and an unleaded fuel. A special test was therefore carried out on leaded *iso*octane for comparison with the test on the base fuel (Fig. 8). The results are shown in Fig. 9.

As before the H.U.C.R. falls in an approximately linear manner with

increasing percentages of argon "air." The difference between the curves for *iso*octane and for *iso*octane + 4 cc T.E.L/I.G. at any given percentage of argon "air" gives the lead response of the fuel when running on an atmosphere containing that percentage of argon "air." It can be seen that in terms of C.R. the difference between the curves decreases with increasing argon "air" content. It is difficult to say, however, whether this represents a genuine reduction in lead response as the value of one C.R. is not the same over the whole H.U.C.R. range.

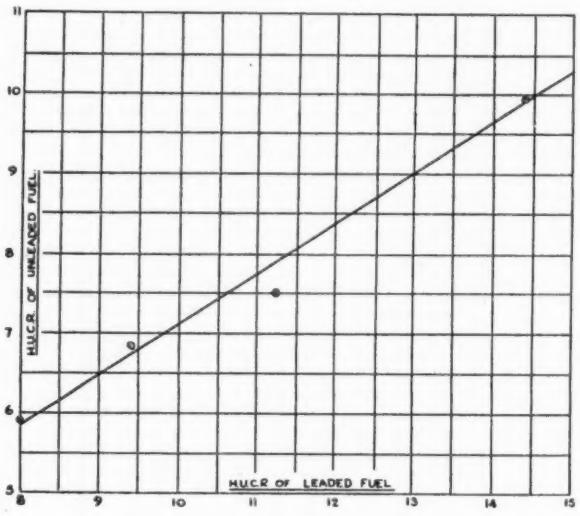

FIG. 10.

EFFECT OF ADDITION OF 4 C.C. TEL/I.G. ON H.U.C.R. OF VARIOUS FUELS.

Maximum knock mixture strength. I.A. optimum for maximum power mixture at each compression ratio.

Accordingly, to enable a more direct comparison to be made, tests were carried out to determine the response of fuels of different initial H.U.C.R. to the addition of 4 cc T.E.L/I.G. Fig. 10 shows an average curve drawn through the points obtained. In Table II an attempt is made to assess the effect of argon on lead response. Columns 1 and 2 were taken from Fig. 10, and columns 3 and 4 from Fig. 9.

TABLE II.

Unleaded fuel H.U.C.R. on normal air.	Leaded fuel H.U.C.R. on normal air.	Percentage of argon "air" to give same H.U.C.R. as col. 1 on *iso*octane.	Leaded fuel H.U.C.R. on argon "air."
8·5	12·25	42	11·0
9·0	13·03	33	11·9
10·0	14·6	16	13·6

Comparing columns 2 and 4, it can be seen that the lead response of a fuel is somewhat less with argon "air" than with normal air, and that this depreciation increases with the argon content of the atmosphere.

"Knock" Tests with Mixtures of Argon "Air" and Carbon Dioxide "Air".

The low specific heat of argon compared with nitrogen introduced an additional factor into the determination of the effect on "knock" of the elimination of nitrogen from the atmosphere. The difficulty was surmounted by using in place of pure argon "air," a mixture of carbon dioxide "air" (high specific heat) and argon "air" (low specific heat) in such proportions as to give as nearly as possible the same thermodynamic properties in the engine as normal air.

In the first place a test was carried out to find a mixture of argon "air" and carbon dioxide "air" which would give the same B.M.P. under comparable conditions in the engine as normal air. A fixed compression ratio of 7·0 and the maximum power mixture strength for normal air were used for this test. The results are plotted in Fig. 11.

It can be seen that a mixture of 65 per cent argon "air" and 35 per cent carbon dioxide "air" gave the same B.M.P. as normal air and nearly the same maximum pressure. The "match air" also had, to all intents and purposes, the same calculated compression pressure and temperature as normal air. A test on the "match air" showed that the ignition advance of 24°E, which was the optimum for normal air, was also the optimum for the "match air."

Table III gives the result of maximum cycle temperature calculations with the various "airs." The method used was that described by Pye.[3]

Table III.

"Air."	Temp. rise ° C (datum 100° C).	No. of mols at max. temp.	Power product.
Normal	2558	65·173	2754
Argon	3202	66·727	3530
Carbon dioxide . .	1857	64·428	1977
Match	2475	65·747	2689

Thus, the maximum cycle temperature is 2658° C for normal air and 2575° C for the "match air," both at chemically correct mixture. The engine power output should theoretically be proportional to :—

$$\frac{\text{No. of mols at maximum temp}}{\text{No. of mols in original mixture}} \times \text{rise in temperature on explosion.}$$

The last column of Table III shows that this factor is 2754 for normal air and 2689 for the "match air." On the basis of this comparison the power obtained with the "match air" should be about 2 per cent less than that obtained with normal air. Factors such as the presence of residual exhaust gas in the working mixture and the richer mixture used at maximum power

conditions have not been taken into account in the above analysis. The agreement between the two is sufficiently close, however, to warrant the conclusion that the " match air " used has, to all intents and purposes, the same thermodynamic properties as normal air in the working range.

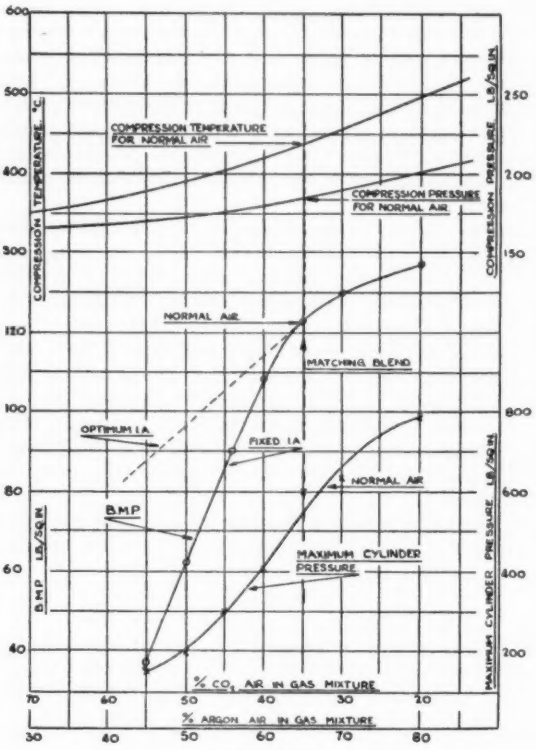

FIG. 11.

MATCHING TESTS.

Fuel.	Test conditions.
Technical *iso*octane.	C.R. 7·0.
S.R. 0·703 at 15° C.	Ign. adv. 24° E.
	Fuel flow for maximum power on normal air.

H.U.C.R.–mixture-strength curves for *iso*octane were now determined both with normal air and with the " match air." The results are plotted in Fig. 12. It can be seen that the H.U.C.R. on " match air " is 0·26 ratios below that on normal air, the fuel flow for maximum knock being 3·98 lb/hr in both cases. Within the limits of error for this type of experiment it may be said, therefore, that the elimination of nitrogen from the induction charge has had no effect on " knock."

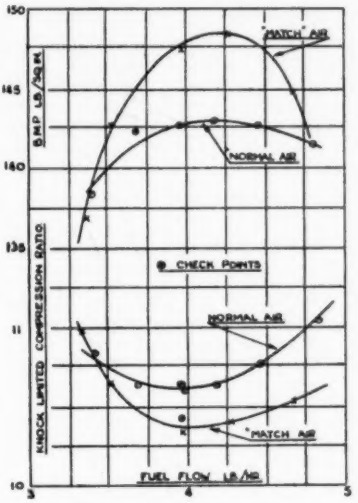

FIG. 12.

COMPARISON OF H.U.C.R. OF ISO-OCTANE ON NORMAL AIR AND ON "MATCH" AIR.
1.A. optimum for maximum power mixture at each compression ratio.

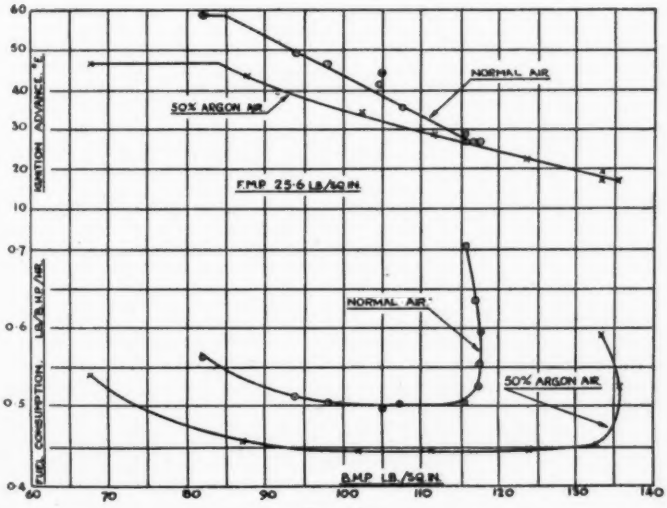

FIG. 13.

COMPARATIVE MIXTURE RANGE LOOPS ON NORMAL AIR AND 50 PER CENT ARGON "AIR."
C.R. 6·5 : 1. Optimum 1.A. Fuel, *iso*octane.

Performance Tests with Argon "Air."

In the course of the experiments, the opportunity was taken of comparing the engine performance when using: (*a*) normal air; and (*b*) a 50/50 mixture of normal air and argon "air." Mixture range loops were obtained at a compression ratio of 6·5, and these have been plotted in Fig. 13. In Fig. 14, they have been replotted against gross fuel flow.

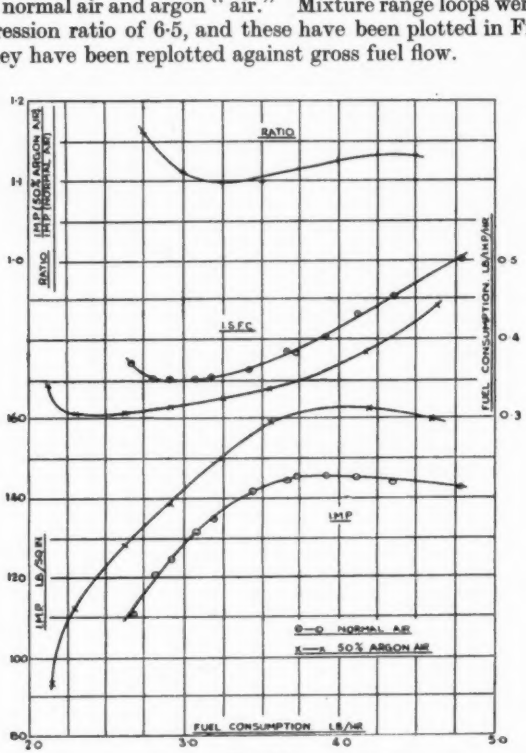

Fig. 14.

Comparative power and fuel consumption curves for normal air and 50 per cent argon "air."

The air standard efficiency for 50 per cent argon "air" is 58·6 per cent compared with 53 per cent for normal air at the same compression ratio (6·5) based on specific heat values at 15° C. The ratio of these two efficiencies is 1·107, which agrees well with the average ratio of the I.M.E.P. and specific fuel consumptions of 1·10.

The optimum ignition advance for maximum power mixtures is less for 50 per cent argon "air" than for normal air. Assuming that for maximum power the maximum cylinder pressure occurs about 12° after top centre, it can be seen that the rate of burning of a 50 per cent argon "air" mixture is $\frac{12 + 26}{12 + 17{\cdot}5} = 1{\cdot}29$ times that of normal air.

Conclusions.

It appears from these tests that nitrogen is not among the prime causes of "knock" in the petrol engine. Its elimination to within 2 per cent of the air charge (the nitrogen being replaced by argon) had no effect *per se* on the tendency to "knock." The change which occurred in the H.U.C.R. of the engine was such as might have been expected from the change in specific heat of the gas charge by the introduction of argon (which has a lower heat capacity than nitrogen).

This was confirmed by carrying out further experiments with a gas mixture of argon, carbon dioxide, and oxygen having the same specific heat and yielding the same power output in the engine as normal atmospheric air. Its general behaviour in rate of burning and in tendency to "knock" was very closely the same as for normal air showing that the absence of nitrogen (or at any rate its reduction to a neligible proportion) had no effect when the complication of difference in specific heat had been removed.

The substitution of argon for nitrogen appears to have had the effect, however, of reducing the effectiveness of lead in suppressing "knock."

This work was carried out in the Ricardo laboratory on behalf of the Shell Petroleum Co. Ltd.

References.

[1] Egerton, A., Smith, F. L., and Ubbelohde, A. R. *Phil. Trans. roy. Soc.*, 1935, **234**, A, 433–52.
[2] Downs, D., and Walsh, A. D. *Nature*, 1949, **163**, 370.
[3] Pye, D. R. "The Internal Combustion Engine," Vol. I.

ADIABATIC AND NON-ADIABATIC RECTIFICATION.

By Kuo-tsung Yu * and James Coull.*

Introduction.

The separation of a mixture at constant pressure is possible only at the expense of some energy. The process of distillation, as one of the many separation processes, is affected by the addition of heat to the system. In the ordinary fractionating column the heat is added to the reboiler so that the liquid is vaporized. The rectifying portion of the column is almost adiabatic so that the vapour is condensed and then revaporized. Such a process is regarded as "adiabatic rectification" in the sense of having an adiabatic rectifying section. This is not the only method, however, of conducting the distillation. The recently developed multiple redistillation process,[1,2,3,4] for example, is a departure from the conventional one. In the multiple redistillation process heat is added and abstracted continuously at the rectifying section. This kind of distillation is regarded as "non-adiabatic rectification."

In the following discussion both cases will be presented as a unit operation from the engineering point of view and as a heat process from the thermodynamic point of view. As classified by the method of operation, the continuous (steady) process is first presented, followed by a consideration of the batch (unsteady) process.

Development of the Process.

Non-adiabatic rectification is a process of distillation consisting essentially of the following units :—

(1) a reboiler for the generation of vapour;
(2) a condenser (total or partial) to supply the reflux;
(3) a column consisting of the following :
  (*a*) one or more heat adding zones in the rectifying section,
  (*b*) one or more heat abstracting zones in the rectifying section.

The conventional rectifying equipment consists only of the first two units plus an adiabatic column. An idealized cascade for the enriching section of the non-adiabatic rectification process is shown in Fig. 1. The vapour generated from the reboiler, B, enters the heat-abstracting unit, C, in which the condensate is returned to the reboiler while the residual vapour rises to the next unit. Since the heat-abstracting unit acts as a "partial condenser," † the residual vapour is enriched. The heat-adding unit, V, receives the liquid reflux from the previous unit and vaporizes

* Department of Chemical Engineering, University of Pittsburgh, Pittsburgh, Pennsylvania.

† The vapour from a conventional partial condenser is in equilibrium with the liquid leaving the condenser, thus accounting for one equilibrum stage. The "partial condenser" considered here can have many equilibrium stages so that the exit vapour and liquid are not in equilibrium with each other.

part of it. The vapour generated from this zone is connected with the residual vapour from the heat-abstracting zone below, while the residual liquid is refluxed back to the reboiler. This mechanism is then repeated until the top is reached.

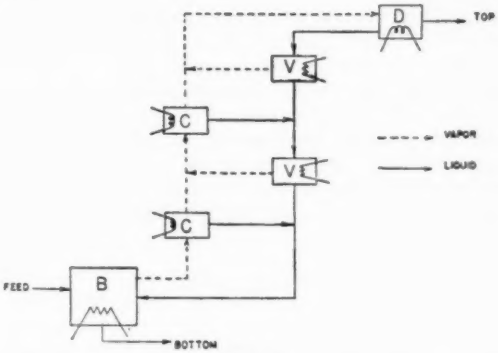

FIG. 1.

IDEALIZED CASCADE FOR THE NON-ADIABATIC RECTIFICATION, ENRICHING SECTION.

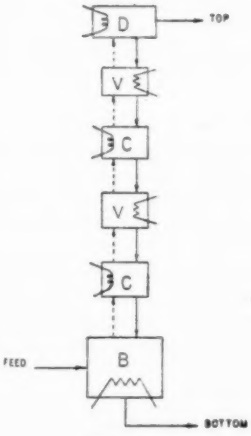

FIG. 2.

IDEALIZED CASCADE FOR THE NON-ADIABATIC RECTIFICATION, SERIES ARRANGEMENT.

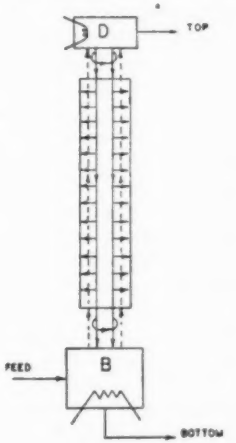

FIG. 3.

IDEALIZED CASCADE FOR THE NON-ADIABATIC RECTIFICATION, PARALLEL ARRANGEMENT.

These units are arranged in a single column and may be classified into two forms :

(a) *Series Arrangement.* In this arrangement the heat-adding units are placed directly above the heat-abstracting units alternating, as shown in Fig. 2. Such a column is analogous in arrangement to the conventional adiabatic plate-type distillation column.

(b) *Parallel Arrangement.* In this arrangement only one heat-adding unit and one heat-abstracting unit are involved, arranged in parallel as shown in Fig. 3. For the convenience of supplying the liquid condensate from the heat-abstracting unit to the heat-adding unit, two concentric tubes are used in a manner such that heat is added to the outer stationary tube while heat is abstracted from the inner rotating tube. Such a column is analogous to the ordinary packed column in the sense that rectification is affected continuously throughout the column.

It is readily seen that the operating principle of the non-adiabatic rectification is basically different from that of the adiabatic column. In the former process, the heat is externally added and abstracted from the rectifying section of the column; while for the latter process, the heat is internally exchanged by vapour–liquid contact.

The wide application of the adiabatic rectification is due mainly to two factors :—

(1) economy of heat exchange (internally);
(2) convenience of operation.

These advantages, however, are completely ruled out where high-vacuum distillation is to be used. Under this condition, the pressure drop through the ordinary plate column or packed column is far greater than the pressure maintained in the still. This leads to the failure of the adiabatic rectification process as employed in the ordinary manner.

Two types of laboratory columns for non-adiabatic rectification have been devised by Dr J. R. Bowman.[1] They have been used effectively in what is termed the multiple redistillation process.

The first column is an open tube with twelve vaporizing–condensing segment pairs. The heat-adding and heat-abstracting zones are alternated, starting with a heat-abstracting zone in the vertical tube above the reboiler. This column, described by Schaffner, Bowman, and Coull,[3] was designed for and restricted in use to high vacuum (0·1 to 0·01 mm Hg) distillation at a throughput rate of about 250 ml/hr. The heat-adding zones are electrically heated, while the heat-abstracting zones are cooled by jets of compressed air. A partial condenser is provided at the top to supply the reflux. The reflux ratio is thus determined by measuring the thickness of the film on the wall of the tube by an optical-glass thickness gauge. The still-pot is electrically heated.

The second type of multiple redistillation column in terms of construction and operation is described by Byron.[4] In this column two concentric tubes are used in which the outer stationary tube is heated and the inner rotating tube cooled. The velocity of rotation is sufficient to throw off centrifugally the condensate which forms on it. The vapour rises in the annular space and tends to condense continuously on the rotor, whereas the reflux and condensate flowing down the inside wall of the outer tube tends to be vaporized continuously. Byron has demonstrated by his operation of this column that good separation can be effected in four systems of wide variety under conditions of atmospheric, intermediate (5 to 15 cm Hg), and low pressure (1 to 0·1 mm Hg).

Determination of Equilibrium Zones.

In the theoretical development to be shown in this section, non-adiabatic rectification is treated from the standpoint of a unit operation of chemical engineering. In this paper, attention is confined only to the first type of multiple redistillation column having the series arrangement of zones. Three major developments are to be considered from the point of view of unit operations :—

(1) The determination of equilibrium stages at finite reflux if the operation is continuous.
(2) The relationship between the continuous and batch operation.
(3) The determination of the minimum number of zones required. This consideration may be used as a guide in column design.

In the following derivation, certain assumptions are made in order to either simplify the derivation or make the derivation possible. It will be necessary to assume a steady operating-point condition and perfect mixing of vapour and of liquid, which seems reasonable for all practical purposes. The assumption of negligible liquid and vapour hold-up in the column is reasonably true for the type of column under consideration. Actual measurement of the thickness of the liquid flowing down the column was shown to be from 0·007 to 0·026 mm.

(a) *Continuous Operation.* As shown in Fig. 2, the material and energy balance relationships for the enriching section consisting of n_v, heat-adding zones, and n_c, heat-abstracting zones, are derived as follows :—

$$V = L + D \quad . \quad . \quad . \quad . \quad . \quad . \quad . \quad . \quad (1)$$

$$Vy = Lx + Dx_D \quad . \quad . \quad . \quad . \quad . \quad . \quad . \quad . \quad (2)$$

$$VH + n_vQ_v = Lh + Dh_D + n_cQ_c + Q_T \quad . \quad . \quad . \quad . \quad (3)$$

If equation (3) is rearranged so that

$$VH = Lh + Dh_D' \quad . \quad . \quad . \quad . \quad . \quad . \quad . \quad (4)$$

where

$$h_D' = h_D + \frac{Q_T + n_cQ_c - n_vQ_v}{D}$$

and

$$Q_T = (\bar{R} + 1)(H_D - h_D)D$$

then

$$h_D' = h_D + (\bar{R} + 1)(H_D - h_D) + \frac{n_cQ_c - n_vQ_v}{D} \quad . \quad . \quad (5)$$

Solving in terms of equations (1), (2), and (4), the " operation equation " is obtained :—

$$y = \frac{h_D' - H}{h_D' - h}\,x + \frac{H - h}{h_D' - h}\,x_D \quad . \quad . \quad . \quad . \quad (6)$$

This relationship can be shown graphically on an enthalpy–concentration diagram similar to the method developed by Ponchon.[5] In this construction, as shown in Fig. 5, the saturated liquid and saturated vapour lines are obtained from thermodynamic data.

The foregoing derivation gives no information on the point-to-point equilibrium composition, but merely shows the liquid composition leaving the zones, and the composition of the vapour entering the same zone. If, according to our assumption, these compositions for any section are maintained constant, then Rayleigh's equation,[6] based on material balances, can be applied. Referring to Fig. 2, at the top heat-adding zone (*i.e.*, where $n_v = 1, n_c = 0$), the following-relationships are obtained :—

$$\ln \frac{L_1}{L_2} = \int_{x_1}^{x_D} \frac{dx}{y - x}$$

but

$$\frac{L_1}{L_2} = \frac{L_1}{L_1 - \frac{Q_v}{\phi}} = \frac{\frac{\overline{R}}{\overline{R}+1} V_t}{\frac{\overline{R}}{\overline{R}+1} V_t - \frac{Q_v}{\phi}} \quad . \quad . \quad . \quad . \quad (7)$$

In order to simplify the expression, two dimensionless groups, the vaporization ratio, β, and the condensation ratio, γ, are introduced and defined as follows :—

$$\beta = \frac{Q_v/\phi}{V_t} = \frac{\Sigma i \beta i}{n_v}$$

$$\gamma = \frac{Q_c/\phi}{V_t} = \frac{\Sigma i \gamma i}{n_c} \quad . \quad . \quad . \quad . \quad . \quad . \quad (8)$$

Equation (7) can be expressed as :—

$$\ln \frac{L_1}{L_2} = \ln \frac{\overline{R}}{\overline{R} - \beta(\overline{R}+1)} = \int_{x_1}^{x_D} \frac{dx}{y - x} \quad . \quad . \quad . \quad (9)$$

By means of equation (9), the composition of the liquid leaving the first heat-adding zone can be evaluated if the y , x data are known. The vapour composition entering this zone can be computed by equation (6).

For the heat-abstracting zone below the first heat-adding zone (*i.e.*, where $n_v = 1$) is obtained by applying Rayleigh's equation

$$\ln \left(\frac{1 - \beta + \gamma}{1 - \beta} \right) = \int_{y_1}^{y_1} \frac{dy}{y - x} \quad . \quad . \quad . \quad . \quad (10)$$

since

$$\frac{V_2}{V_1} = \frac{V_t - \frac{Q_v}{\phi} + \frac{Q_c}{\phi}}{V_t - \frac{Q_v}{\phi}} = \frac{1 - \beta + \gamma}{1 - \beta}$$

By means of equation (10), the vapour composition entering the heat-abstracting zone can be obtained. The liquid composition leaving this zone can then be calculated by equation (6).

Similarly, at the n^{th} heat-adding zone (*i.e.*, where $n_v = n$), is obtained :—

$$\ln \frac{\overline{R} - (n-1)(\beta - \gamma)(\overline{R}+1)}{\overline{R} - [(n-1)(\beta - \gamma) + \beta](\overline{R}+1)} = \int_{x_n}^{x_{n-1}} \frac{dx}{y - x} \quad . \quad (11)$$

At the n^{th} heat-abstracting zone (*i.e.*, where $n_c = n$) is obtained :—

$$\ln \frac{1 - n(\beta - \gamma)}{1 - (n-1)(\beta - \gamma) - \beta} = \int_{y_{n+1}}^{y_n} \frac{dy}{y - x} \quad . \quad . \quad . \quad (12)$$

By means of equations (6), (11), and (12), the number of equilibrium heat-adding and heat-abstracting zones can, therefore, be evaluated. The graphical representation shown in Figs. 4 and 5 is for the special case where $Q_v = Q_c$ (*i.e.*, where $\beta = \gamma$). For the general case where the heat effects are not equal (*i.e.*, where $Q_v \neq Q_c$) a more complex diagram is obtained which is omitted in this paper in the interest of conserving space.

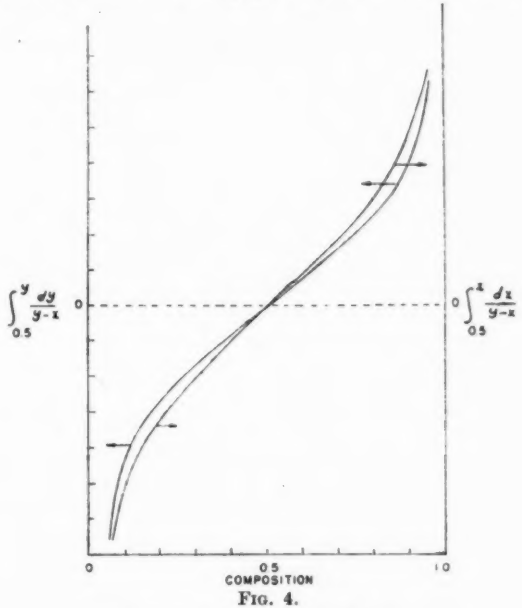

FIG. 4.

REPRESENTATION OF RAYLEIGH'S EQUATION.

Referring to Fig. 4, the value of the integrals in equations (11) and (12) as obtained from the equilibrium data are plotted against the composition, x or y, so that two curves are obtained.

The curves in this diagram may be characterized as the "pseudo-equilibrium curves" for the separation. In Fig. 5 these two curves are drawn separately so that the upper curve represents the vapour phase

i.e., $$\int_{y}^{0.5} \frac{dy}{y - x} \; vs \; . \; y$$

and the lower curve represents the liquid phase

i.e., $$\int_{x}^{0.5} \frac{dx}{y - x} \; vs \; . \; x$$

The middle portion of the diagram in Fig. 5 shows an enthalpy–concentration plot representing the relationship expressed by equation (6). The procedure of construction is as follows. Locate the points representing the feed, F, the top product, D, and the bottom product, B, for the specified

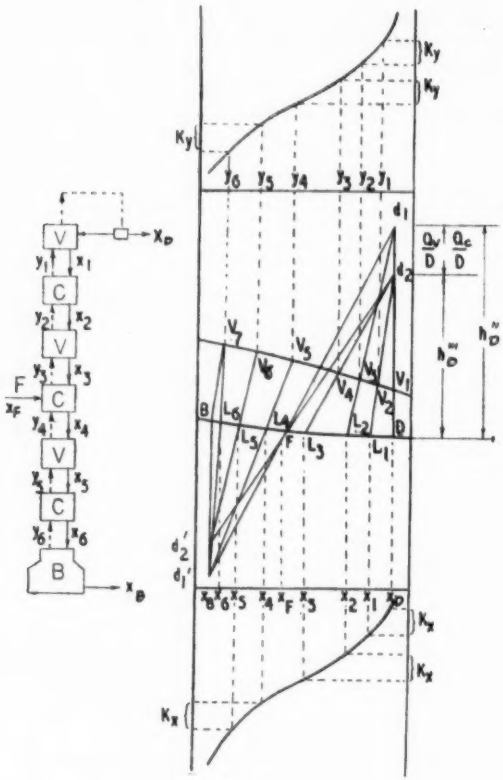

FIG. 5.
GRAPHICAL SOLUTION.

separation in terms of composition and enthalpy. If the reflux ratio is known, the operating point d_1 can be located on the line $x = x_D$ such that :—

$$h_D'' = h_D + (\overline{R} + 1)(H_D - h_D)$$

Another operating point d_2 is also located on $x = x_D$ such that :—

$$h_D''' = h_D'' - \frac{Q_v}{D}$$

The points d_1' and d_2' are projected on the vertical line, $x = x_B$, through

F, as shown. It should also be noted that, under this condition, equations (11) and (12) reduce to give :—

$$\ln \frac{\overline{R}}{\overline{R} - \beta(\overline{R}+1)} = \int_{x_n}^{x_{n-1}} \frac{dx}{y-x} = K_x \quad . \quad . \quad . \quad (11')$$

$$\ln \frac{1}{1-\beta} = \int_{y_{n+1}}^{y_n} \frac{dy}{y-x} = K_y \quad . \quad . \quad . \quad . \quad (12')$$

Starting from the heat-adding zone below the condenser, the liquid composition entering this zone is represented by x_D. A vertical line, $x = x_D$, is projected to the x curve at the lower part of the diagram. A distance equal to K_x (which is calculated from the left-hand side of equation (11')) is measured and projected back to the curve so that the liquid composition leaving this zone, x_1, can be read. The relationship between y_1 and x_1 is represented by equation (6); or in other words, by the line $d_2V_2L_1$. From V_2 the vapour composition leaving the first heat-abstracting zone, y_1, is located. Project y_1 to the y-curve at the upper part of the diagram and obtain the vapour composition entering this zone, y_2, by measuring the distance K_y as was done for K_x. The relationship between y_2 and x_2, the liquid composition leaving the first heat-abstracting zone from the top, is given by equation (6); or in other words, the line $d_1V_3L_2$. Similar steps are then constructed until the feed F is reached. After passing through the feed point F, the lower operating points d_1' and d_2' are used. The points d_1 and d_1' are used for the heat-abstracting zones, while the points d_2 and d_2' are used for the heat-adding zones. The detailed relationship is shown in Fig. 5, where the feed is introduced to the column between y_3 and y_4. In the final step a tie line V_7B is drawn, since y_6 is in equilibrium with x_B for a perfect reboiler.

(b) *Batch Operation.* In a batch operation, the reflux ratio and the top-product composition cannot be kept constant simultaneously. The discussion will be confined to the two following cases :—

(1) constant product composition with variable reflux;
(2) constant reflux with variable top product composition.

In the following treatment, we shall confine our consideration to the case where $Q_v = Q_c$. The basic material and heat-balance equations for the batch operation are as follows :—

$$F = P + W \quad . \quad . \quad . \quad . \quad . \quad . \quad . \quad (13)$$

$$Fx_F = Px_D + Wx_B \quad . \quad . \quad . \quad . \quad . \quad . \quad . \quad (14)$$

$$q = [(\overline{R}+1)\phi + (h_D - h_B)]\frac{dP}{d\theta} = V_t\phi \quad . \quad . \quad . \quad (15)$$

Equations (13), (14), and (15) can be solved given the following equation for constant x_D and variable $\overline{R}$:—

$$-\int_{x_F}^{x_w} \frac{(\overline{R}+1)}{(x_D - x_B)^2}\, dx_B = \frac{V_t}{F(x_D - x_F)}\theta \quad . \quad . \quad . \quad (16)$$

and for the operation where $\overline{R}$ is a constant but both x_D and x_B are variable, one obtains :—

$$\int_{x_{D_1}}^{x_{D_2}} \frac{x_B - x_F}{(x_B - x_D)^2}\, dx_D + \int_{x_{B_1}}^{x_{B_2}} \frac{x_F - x_D}{(x_B - x_D)^2}\, dx_B = \frac{V_t}{\overline{R} + 1}\,\theta \quad . \quad (17)$$

Both equations (16) and (17) can be integrated graphically by calculating the instantaneous relationship between x_B and x_D from their initial to their final values.

(c) *Determination of Minimum Number of Zones.* The purpose of this derivation is to calculate the minimum number of heat-adding and heat-abstracting zones required for a specific separation. In the continuous operation, the minimum number of zones is determined under the condition of total reflux. In the batch operation where a constant reflux is used, the minimum number of zones required does not provide significant information; but for the operation where a constant top-product composition is obtained, the minimum number of zones required is fixed by the conditions at the end of the distillation where the bottom composition is leanest and the reflux becomes total. In other words, the load of separation is at a maximum. Since at total reflux,

$$R = \infty$$

equations (11′) and (12′) become, for $n_v = 1$, $n_c = 0$,

$$\ln \frac{1}{1 - \beta} = \int_{x_1}^{x_D} \frac{dx}{y - x}$$

For $n_v = 1$, $n_c = 1$,

$$\ln \frac{1}{1 - \beta} = \int_{y_1}^{y_1} \frac{dy}{y - x}\,.$$

At the bottom of a column with n pairs of heat-adding and heat-abstracting zones (*i.e.*, $n_v = n$, $n_c = n$), is obtained :—

$$\ln \frac{1}{1 - \beta} = \int_{y_n}^{y_{n-1}} \frac{dy}{y - x}$$

Combining all the equations,

$$2(n)_{\min.} \ln \frac{1}{1 - \beta} = \int_{x_1}^{x_D} \frac{dx}{y - x} + \int_{y_2}^{y_1} \frac{dy}{y - x} + \ldots + \int_{y_n}^{y_{n-1}} \frac{dy}{y - x} \quad . \quad (18)$$

The right-hand side of equation (18) can be evaluated, in general, by graphical integration from the x , y equilibrium data. Since most of the systems to be fractionated are under reduced pressure, the relative volatility is constant.[7] One can, therefore, integrate approximately by the following treatment. Under the assumption of constant α, the following approximation can be made :—

$$\int_{x_1}^{x_D} \frac{dx}{y - x} + \int_{y_2}^{y_1} \frac{dy}{y - x} + \ldots + \int_{y_n}^{y_{n-1}} \frac{dy}{y - x} = \int_{y_1}^{y_D} \frac{dy}{y - x} + \int_{x_2}^{x_1} \frac{dx}{y - x} + \ldots + \int_{x_n}^{x_{n-1}} \frac{dx}{y - x} \quad . \quad (19)$$

In actual computation of the values for both sides of equation (19), a very close check has been obtained. Since it is obvious that

$$\left[\int_{x_1}^{x_D}\frac{dx}{y-x}+\int_{x_2}^{x_1}\frac{dx}{y-x}+\ldots.+\int_{x_n}^{x_{n-1}}\frac{dx}{y-x}\right]+\left[\int_{y_1}^{y_D}\frac{dy}{y-x}+\int_{y_2}^{y_1}\frac{dy}{y-x}+\ldots.+\int_{y_n}^{y_{n-1}}\frac{dy}{y-x}\right]=\int_{x_n}^{x_D}\frac{dx}{y-x}+\int_{y_n}^{y_D}\frac{dy}{y-x} \quad . \quad (20)$$

The right-hand side of equation (20) can be integrated to give the following expression under total reflux where $x_D = y_D$ and $x_n = y_n$:—

$$\int_{x_n}^{x_D}\frac{dx}{y-x}+\int_{y_n}^{y_D}\frac{dy}{y-x}=\frac{\alpha+1}{\alpha-1}\ln\left(\frac{y_D}{1-y_D}\right)\left(\frac{1-y_n}{y_n}\right) \quad . \quad (21)$$

Combining equations (18), (19), (20), and (21), is obtained :—

$$2(n)_{\min.}\ln\frac{1}{1-\beta}=\tfrac{1}{2}\left(\frac{\alpha+1}{\alpha-1}\right)\ln\left(\frac{y_D}{1-y_D}\right)\left(\frac{1-y_n}{y_n}\right)$$

Replacing y_n by y_B, the composition of vapour from the reboiler, the minimum pairs of zones required, n, is found to be :—

$$(n)_{\min.}=\frac{\tfrac{1}{2}\left(\frac{\alpha+1}{\alpha-1}\right)\ln\left(\frac{y_D}{1-y_D}\right)\left(\frac{1-y_B}{y_B}\right)}{\ln(\beta-1)} \quad . \quad . \quad . \quad (22)$$

Equation (20) also gives an interesting result in comparison with Fenske's equation [8] for the determination of the minimum number of theoretical plates in an adiabatic fractionating column. Fenske's equation is written as :—

$$N=\frac{1}{\ln\alpha}\ln\left(\frac{y_D}{1-y_D}\right)\left(\frac{1-y_B}{y_B}\right) \quad . \quad . \quad . \quad . \quad (23)$$

By the expansion of the logarithm series, when the value of α is less than 1·5, is obtained :—

$$\ln\alpha=2\left(\frac{\alpha-1}{\alpha+1}\right)$$

Under the condition that each zone is equivalent to one theoretical plate, *i.e.*, when $n = 2N$, the following relationship should be fulfilled by combining equations (22) and (23),

$$\ln(\beta-1)=1$$

or

$$\beta=e+1$$

Or, in other words, the amount of heat added or subtracted from each zone should be equal to 3·7 times the total condenser load.

Thermodynamic Consideration.

The statement [9] has been made that the minimum work required for continuous separation is that based on the isothermal process on the

assumption that the vapour and the liquid behave ideally. If Raoult's law is valid, the minimum work, W_T, necessary for the complete separation of one mole of feed in a continuous process is given as :—

$$-W_T = -RT[x_F \ln x_F + (1 - x_F) \ln (1 - x_F)] \quad . \quad . \quad (24)$$

This isothermal criterion is evidently not a fair basis for the comparison of separation efficiency. Thermodynamically, equation (24) deals with a continuous reversible process, but no distillation process, actual or theoretical, can be conducted reversibly due to the fact that there is a net loss of availability.

The minimum work required for a non-isothermal separation obviously cannot be represented by equation (24). In order to evaluate the minimum work, the concept of " Process Column " is developed so that the distillation process, as defined, is operated with minimum energy requirement

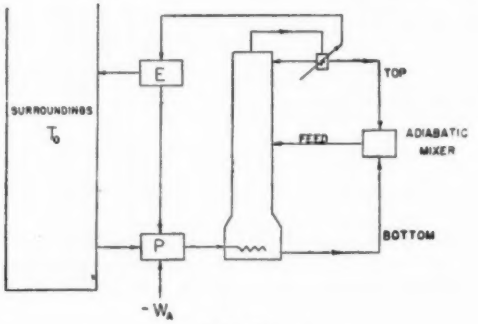

FIG. 6.
SECOND LAW ANALYSIS OF ADIABATIC RECTIFICATION.

and maximum efficiency. In this process column, in general, the following conditions apply :—

(1) Perfect column construction, *i.e.*, the radiation effects, fluid-flow friction, etc., will be ruled out.

(2) All the heat is added and abstracted reversibly. In other words, the irreversibility is not from the heat transfer but from the process itself.

(3) All the heat energy is taken and exhausted to an infinite heat reservoir, the surroundings, by means of a Carnot heat pump and heat engine. The work obtained from the Carnot heat engine is then used as a part of the energy necessary to operate the heat pump. The minimum work for the separation, therefore, represents the other part of the energy required to operate the heat pump.

(4) The column is operated at constant pressure. This condition is important because no separation is possible at constant pressure without maintaining a temperature difference between the top and the bottom products.

There are two kinds of process columns—adiabatic and non-adiabatic. The adiabatic process column, as shown in Fig. 6, consists of a total condenser, adiabatic rectifying section, and a reboiler. In order to complete

a cycle for the separation, an adiabatic mixer is provided. In Fig. 6, the heat added to the reboiler is by means of a Carnot heat pump receiving the heat at the surrounding temperature, T_0, and delivering heat at the bottom temperature, T_s. The heat removed from the condenser at the top temperature, T_c, is used to drive the Carnot heat engine and then exhausted to the surroundings. The top and bottom products are mixed and recycled for separation. The work required for the separation by this process is then

$$-W_A = \text{work to the Carnot heat pump—work done by the Carnot heat engine}$$

$$= \frac{q}{T_s}(T_s - T_0) - \frac{Q_T}{T_c}(T_c - T_0)$$

$$= (T_s - T_0)\Delta S_s - (T_c - T_0)\Delta S_T \quad . \quad . \quad . \quad . \quad (25)$$

By taking a heat balance,

$$q = Q_T$$

Equation (25) then becomes

$$-W_A = T_0 q\left(\frac{1}{T_c} - \frac{1}{T_s}\right)$$

$$= T_0 \Delta S_A \quad . \quad . \quad . \quad . \quad . \quad . \quad . \quad . \quad (26)$$

Equation (26) is analogous with the change of availability as originally defined by Keenan.[10] The concept of availability, however, can be extended in a more generalized sense to be defined in an "energy flow process" with no flow work as :—

$$-\Delta B = T_0(\Sigma S_l - \Sigma S_e) \quad . \quad . \quad . \quad . \quad . \quad (27)$$

where ΣS_l and ΣS_e represent the summation of the entropy leaving and entering the system respectively. Comparing equations (26) and (27), one can conclude that the minimum work required for separation is equal to the decrease of availability in this process, or,

$$-W_A = -\Delta B_A \quad . \quad . \quad . \quad . \quad . \quad . \quad . \quad . \quad (28)$$

The non-adiabatic process column is shown in Fig. 7. The heats abstracted, Q_T and Q_c, are transferred reversibly to the surrounding temperature, T_0, through the Carnot heat engines. The Carnot heat pumps deliver the heat at the elevated temperature from the temperature of the surroundings, T_0, in the case of q and Q_v. In Fig. 7, E represents the Carnot engine, while P represents the heat pumps. The net work required for the separation by this process $-W_{NA}$ is then :—

$$-W_{NA} = \Sigma \text{ work to the Carnot heat pumps} - \Sigma \text{ work done by the Carnot heat engine.}$$

$$= \frac{q}{T_s}(T_s - T_0) + \Sigma \int_1^2 \frac{T - T_0}{T}\, dQ_v - \frac{Q_T}{T_c}(T_c - T_0) - \Sigma \int_1^2 \frac{T - T_0}{T}\, dQ_c$$

$$= T_0(\Delta S_T + \Sigma \Delta S_v - \Delta S_s - \Delta S_c)$$

$$= -\Delta B_{NA} \quad . \quad . \quad . \quad . \quad . \quad . \quad . \quad . \quad . \quad . \quad . \quad . \quad (29)$$

Equations (28) and (29) provide a thermodynamic basis to calculate the minimum work for the separation. The evaluation, generally, should be done by graphical integration. The detailed discussion will be omitted in this paper. It will be of interest to present the results of using equations (28) and (29) under the condition where the mixture to be separated is a closely boiling binary with a constant relative volatility, α. It has been shown that the minimum work required for separation in this case is given as :—

$$-W_A = \frac{T_0 R}{2} \frac{(x_D - x_B)^2}{x_B} D \quad . \quad . \quad . \quad . \quad . \quad (30)$$

$$-W_{NA} = \frac{T_0 R}{2} \left[\frac{(x_D - x_B)^2}{x_B} + (x_D - x_B) \bar{R}_m (\alpha - 1) \right] D$$

(when $Q_v = Q_c$) . . (31)

A new concept of the thermodynamic efficiency of distillation has also been developed based on the consideration of minimum work.[11]

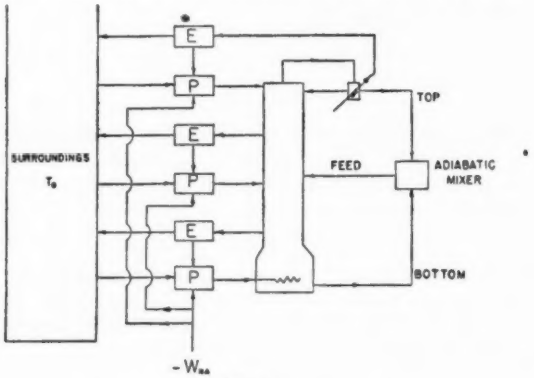

FIG. 7.

SECOND LAW ANALYSIS OF NON-ADIABATIC RECTIFICATION.

CONCLUSION.

The process of distillation is classified into two types—the adiabatic and the non-adiabatic rectification. The process of non-adiabatic rectification is described and developed from two different points of view as a distillation process in unit operations and as a heat process in thermodynamics. The method of calculating the number of heat-adding and heat-abstracting zones for continuous and batch operation and the calculation of the minimum number of zones required are presented. The thermodynamic basis of formulating the minimum work required for the adiabatic and non-adiabatic rectification is outlined by applying the principles of the second law.

ACKNOWLEDGMENT.

The authors wish to express their appreciation to Dr J. R. Bowman, Mellon Institute, Pittsburgh, Pennsylvania, inventor of the multiple

redistillation process, for his constructive criticism and encouragement during the progress of this research at the University of Pittsburgh.

Nomenclature.

B = rate of bottom product removal.
ΔB = increase of availability. Subscript A refers to adiabatic and subscript NA refers to non-adiabatic rectification.
D = rate of top product removal.
F = total amount of original charge.
h = enthalpy of liquid at any section. Subscript D refers to top liquid product, and subscript B refers to bottom liquid product.
H = enthalpy of vapour at any section. Subscript D refers to the vapour entering the total condenser.
L = rate of liquid throughout.
n = number of zones. Subscript c refers to heat-abstracting zones and subscript v refers to heat-adding zones.
$n_{\text{min.}}$ = minimum number of *pairs* of heat-adding and heat-abstracting zones.
N = minimum number of theoretical plates in an adiabatic rectification process.
P = total amount of top product.
q = rate of heat added to reboiler.
Q = rate of heat transferred. Subscript c refers to heat abstracted from a heat-abstracting zone; subscript T refers to heat abstracted from total condenser and subscript v refers to that added to a heat-adding zone.
R = gas law constant.
$\overline{R}$ = reflux ratio. Subscript n refers to the minimum reflux.
ΔS = increase of entropy. Subscript A refers to adiabatic rectification; subscript c refers to heat-abstracting zone; subscript NA refers to non-adiabatic rectification; subscript s refers to reboiler; subscript T refers to total condenser; and subscript v refers to heat-adding zone.
T = absolute temperature. Subscript c refers to total condenser; subscript s refers to reboiler; and subscript o refers to surroundings.
V = rate of vapour throughput. Subscript t refers to top throughput.
W = amount of residue in the reboiler.
w = work done by the system on the surroundings. Subscript A refers to adiabatic rectification; subscript NA refers to non-adiabatic rectification and subscript T refers to isothermal separation.
x = liquid composition. Subscript B refers to bottom product; subscript D refers to top product; subscript F refers to feed; and subscript w refers to final residue in reboiler.
y = vapour composition. Subscript B refers to the vapour generated from the reboiler and subscript D refers to the vapour entering the total condenser.
a = relative volatility.
ϕ = average latent heat of vaporization.
θ = time.

(Subscript 1 refers to initial condition and subscript 2 refers to final condition throughout all the nomenclature.)

References.

[1] Bowman, J. R. Mellon Institute of Industrial Research, Pittsburgh, Pa. Patents applied for in name of Dr J. R. Bowman.
[2] Schaffner, R. M. Thesis in Chemical Engineering, University of Pittsburgh, 1941.
[3] Schaffner, R. M., Bowman, J. R., and Coull, J. *Trans. Amer. Inst. chem. Engrs*, 1943, **39**, 77.
[4] Byron, E. S. Thesis in Chemical Engineering, University of Pittsburgh, 1945.
[5] Ponchon. *Tech. Moderne*, 1921, **13**, 20.
[6] Rayleigh. *Phil. Mag.*, 1905, **4**, Sixth Series.
[7] Bishop, C. A. Thesis in Chemical Engineering, University of Pittsburgh, 1942.
[8] Fenske. *Industr. Engng Chem.*, 1932, **24**, 482.
[9] Weber, H. C., and York, R., Jr. *Trans. Amer. Inst. chem. Engrs*, 1938, **34**, 569.
[10] Keenan, J. H. *Mech. Engr*, 1932, **54**, 195.
[11] Yu, K. T. Thesis in Chemical Engineering, University of Pittsburgh, 1947.

THE SHELL-RICARDO LUBRICATING-OIL TEST ENGINE.

By D. Downs * (Assoc. Fellow).

Introduction.

A good indication of the intrinsic lubricating properties of an oil may be gained from laboratory physical tests and from simple mechanical rig tests. An oil has to do rather more than perform a purely lubricating function, however. In the process of lubricating and cooling the engine, the oil is subjected to high temperatures in the cylinder and also to contamination from the products of decomposition of the fuel, from the atmosphere, and from the products of wear of the engine parts themselves.

Deterioration of an oil in this way results in the formation of carbonaceous deposits and lacquer on the piston, and of sludge in the crankcase. This may lead to trouble in service due to blocking of oilways, sticking of valves, and the sticking of piston-rings in their grooves. The oil may also develop acidity and cause corrosion of engine parts.

It is not easy to assess the ability of an oil to resist oxidation and deterioration arising from products of combustion by any laboratory test. In fact, no laboratory oxidation test has yet been devised which will satisactorily predict the behaviour of an oil in service. Ideally this would be done by testing the oils in engines under actual service conditions. Such tests would, however, be both lengthy and costly, and the difficulty of reproducing the operating conditions would make accurate comparative work almost impossible. For this reason accelerated engine tests, *i.e.*, tests on engines in which the conditions of load and temperature have been so increased in severity as to produce the effect of, say, 1000 hr running in 50 to 100 hr are the more usual solution adopted for routine rating within the industry.

The only recognized standard engine tests for diesel lubricating oils in general use at present are those required for the U.S. Army Specification 2104B and the U.S. Navy 9000 series for high-duty lubrication. They are, of course, of American origin and require test engines, Caterpillar, Chevrolet, or G.M. Diesel, of American manufacture. These engines are not easy to obtain in the United Kingdom, and are not necessarily representative of British practice. In addition, the tests themselves, with the possible exception of the L5, are not entirely suitable for rating modern heavy duty oils. The need has therefore been felt for some time for a British lubricating-oil test engine of such a type that would enable a wide range of tests to be carried out on the one unit. These tests, while being generally similar in nature to the L series, would in all probability involve more severe conditions of load and temperature to cover future developments in lubricants and service requirements.

It was to meet this need that the Shell Petroleum Co., Ltd., and Ricardo & Co. Engineers (1927), Ltd., co-operated in the design and manufacture

* Fuel Research Engineer, Ricardo & Co., Engineers (1927) Ltd.

of a suitable engine under the aegis of the Engine Tests of Lubricants Panel of the Institute of Petroleum. Two engines of this type have already been manufactured, and one has successfully completed a 100-hr type test at the Thornton Research Centre.

The Design Specification of the Engine.

The prime requisites for a lubricating-oil test engine are the greatest possible flexibility of operating conditions, consistency of performance, and ease of access to all important parts for cleaning and inspection. These considerations formed the basis of the design specification of the engine which was drawn up as follows. The principle requirements were that :—

1. The engine should embody a crankcase–crankshaft assembly on to which could be bolted various types of cylinder. Thus the possible range of tests would be large, and the number of different oil-testing engines now in use could be reduced.
2. The crankcase–crankshaft assembly should be of sturdy construction to enable it to operate satisfactorily for long hours at the high outputs visualized for these tests and should be such that with a wet sump efficient lubrication could be obtained with not more than 2 gal of oil.
3. Dismantling and assembly of the unit should be easily accomplished. It should be possible to exchange the various cylinder assemblies rapidly and to remove the piston from the connecting-rod without disturbing the big-end bearing.
4. The piston temperature control should be accurate, as the ring-belt temperature will largely influence the ring-sticking and carbon-forming tendencies of the oil.
5. The oil-circulation system should consist of two distinct circuits, one supplying the valve cams and timing gears with a straight mineral oil, and the other supplying the test oil to the rest of the engine, the supply cooling the piston being capable of separate control. Separation of the oil circuits in this way would, of course, facilitate the cleaning of the engine between tests, as it would obviate the necessity of disturbing the parts of the engine lubricated by the straight mineral oil.
6. The internal surface of the crankcase and various oil-ways should be smooth and free from pockets.
7. Combined copper in bearing metals would be allowed, but otherwise copper and copper alloy should not be used owing to their catalytic effect on lubricating-oil deterioration. For this reason all the oil-pipe work and the gear pumps should be of ferrous material.
8. Knowledge of the temperatures at various points in the engine is very important, and reasonable provision should be made for thermocouples in the piston, cylinder-liner, crankpin, and main bearings.

The engine was designed with the following maximum performance requirements in view. It is, of course, unlikely that all extremes of performance will be required simultaneously.

Speed :	normal *c.* 1200 r.p.m., maximum 2000 r.p.m.
Load :	maximum 300 p.s.i. b.m.e.p. at 1200 r.p.m.
Duration :	500 hr
Coolant temperatures :	of the same order of magnitude as those specified for the L series of tests.

Description of the Engine.

The unit is designed with a stroke of 6 in, which size enables a large selection of typical modern high-speed diesel-engine cylinders to be fitted to the one crankcase. So far two combustion systems, direct injection and compression swirl, both of $4\frac{1}{4}$-in bore, have been run in the engine, and a two-stroke system has been designed but not yet tested.

Figs. 1 and 2 show the universal crankcase section, the internal surface of which is shot-blasted to a smooth finish to enable it to be cleaned easily. The crankshaft is made of Mechanite cast iron, and is supported by two main bearings consisting of steel shells lined with white metal. The bearing housings are designed so as to allow the crankshaft to be removed without disturbing the bearings. Two removable rollers have been provided to support the crankshaft when this operation is being carried out.

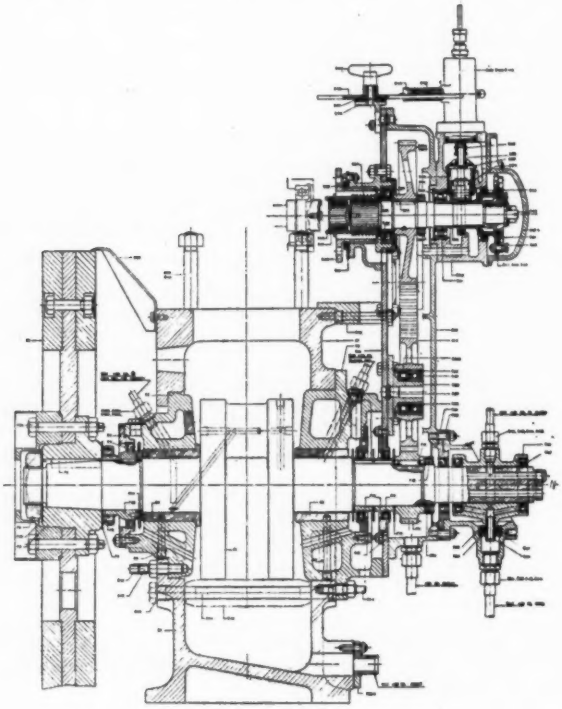

FIG. 1.

UNIVERSAL CRANKCASE SECTION.

The flywheel has been made so that the outer rim and web can be removed from the inner boss, thus allowing the whole crankshaft assembly to pass through the crankcase.

The big-end bearing consists of two half shells, the top half being lined with 70/30 copper–lead, and the bottom half with white metal. The connecting-rod is of H section 0·45 carbon steel, and is interchangeable between the various types of cylinder. The small-end bearing consists of a fully floating plain *Y* alloy bearing running in a hardened-steel bush.

The drive to the camshaft is through a train of gears driven from the front end of the crankshaft. From the spindle of the top timing gear the

drive is taken through an internally splined sleeve to the camshaft. This sleeve can be disengaged and held with a spring clip so that it does not impede the removal of the cylinder. Some variation in the valve timing can be obtained by suitable adjustment of this sleeve and the timing gear, the minimum change which it is possible to make being 3·8 crank degrees.

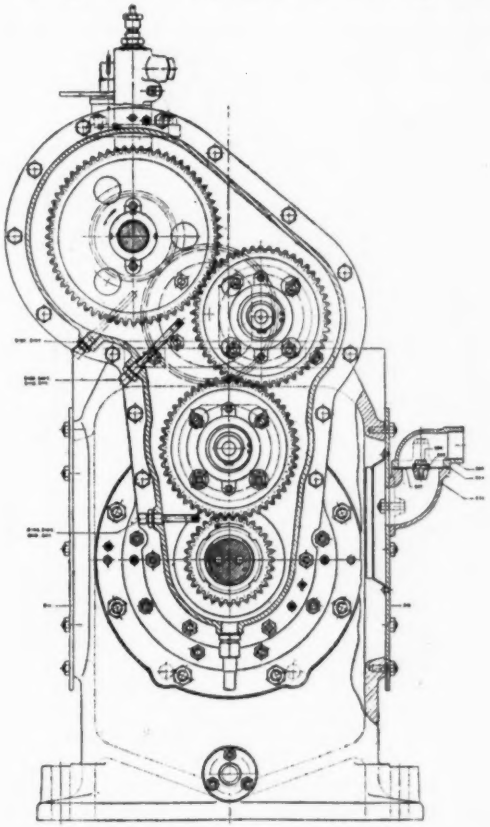

FIG. 2.

END GEAR ARRANGEMENT OF CRANKSHAFT SECTION.

The other end of the timing-gear spindle drives the fuel-pump cam. The fuel-pump itself is of the flange type (C.A.V. Type No. BBF IB70B03) without advance and retard mechanism. The pump timing can be adjusted statically by rotating the outer sleeve, which forms part of the pump camshaft, relative to the inner shaft, these two members being secured by locking the two end plates together. These plates are drilled with two series of holes which give a vernier adjustment. The minimum variation obtainable by adjustment of the relative positions of these two

plates is 2·6 crank degrees. A fine adjustment can also be obtained by alteration of the pump tappet.

The lubricating-oil system is divided into two main circuits, one supplying the camshaft, the fuel-pump cam, and the timing gears with a straight mineral oil, and the other supplying the test oil to the main bearings, big-end, and rockers.

The mineral oil is fed directly to each place, and is allowed to flow by gravity down the inside of the timing case to an outlet at the bottom. Each pair of timing gears has its own individual supply.

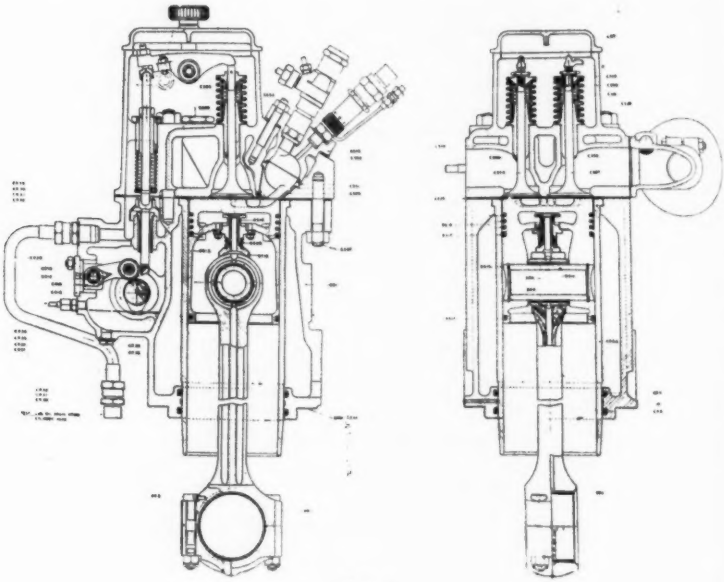

FIG. 5.

RICARDO COMET MARK III CYLINDER AND HEAD.

The test oil is supplied to each individual main bearing from a common source, the flywheel-end inlet also feeding the big-end bearing. The oil flowing from the rockers to the sump by-passes the cambox through an external pipe to avoid contaminating the gear oil. In order that oil from one circuit should not pass into the other circuit, each system is isolated by a number of Super oil seals fitted along the crankshaft.

To avoid passing the piston cooling oil through the main bearing and to enable an accurate control to be obtained, a separate feed has been arranged to supply oil to the piston. The oil is fed into a fully floating " banjo " fitting on the timing end of the crankshaft from which it passes through the crankshaft and crankpin up the connecting-rod to the piston. This oil as well as that supplied to the main bearings, big-end, and rockers, is scavenged from the base of the crankcase.

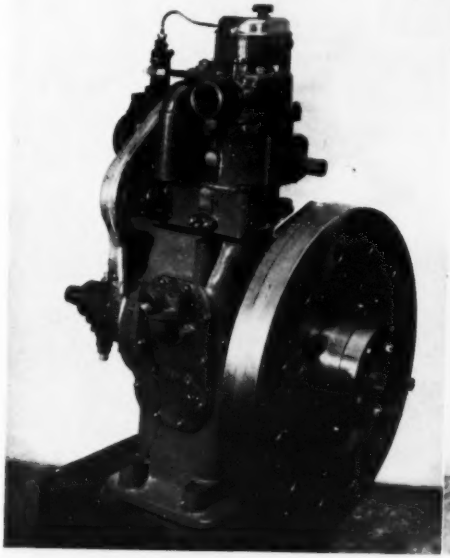

FIG. 3.

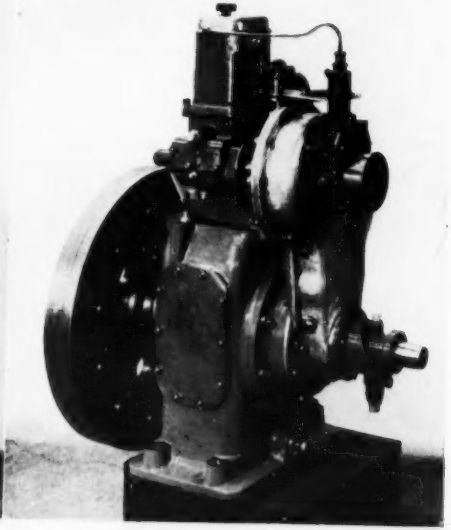

FIG. 4.

COMPLETE ENGINE ASSEMBLED WITH DIRECT-INJECTION CYLINDER AND HEAD.

[To face p. 788.

Figs. 3 and 4 show the engine assembled with a proprietary direct-injection combustion system. Figs. 5 and 6 show the Ricardo Comet Mk. III cylinder-block and head specially designed for this unit.

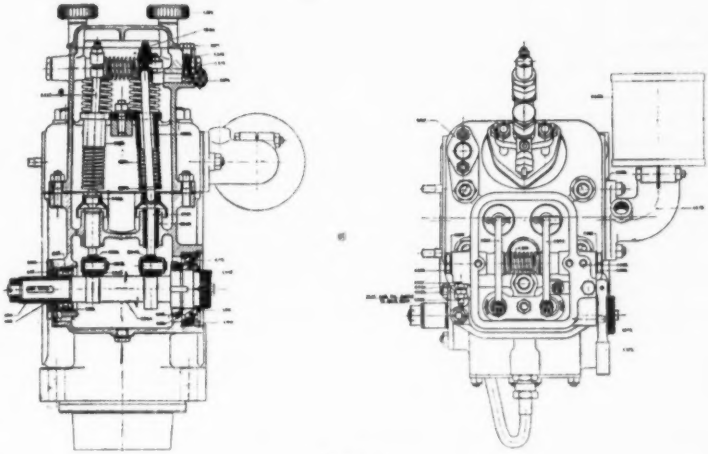

FIG. 6.

CAMSHAFT AND VALVE GEAR, RICARDO COMET MK III.

THE PERFORMANCE OF THE ENGINE.

The performance of the engine depends, of course, on the particular combustion system with which it is fitted. Thus, of the two cylinders so far tested, the direct injection and the Comet Mk. III, both have given the expected power output and fuel consumption on an indicated basis. The brake performance figures on the S-R crankcase are necessarily somewhat low because of the relatively high friction losses of the unit. These high friction losses are an inevitable accompaniment of the larger bearing areas necessary to ensure complete mechanical reliability under all conditions of load and speed. The oil seals on the crankshaft provide an additional source of loss. From the point of view of the rating of the oil, however, it is the indicated performance of the engine which is important.

The crankcase fitted with the direct-injection combustion system has now completed a 100-hr type test at 1600 r.p.m. and 83 p.s.i. b.m.e.p., equivalent to 115 p.s.i. i.m.e.p. or to 90 p.s.i. b.m.e.p. on the usual industrial single-cylinder crankcase. All moving parts were found to be in perfect condition at the conclusion of this test.

It is satisfactory to note that the oil seals gave good service at oil inlet temperatures up to 100° C. Tests have not yet been carried out at higher temperatures but, if this design should prove unsuitable under these conditions, mechanical seals of the piston-ring type are available.

All the running spares of the direct-injection version are of proprietary

manufacture and are readily available in large numbers, a fact of considerable importance in routine engine test work.

The mechanical reliability of the design having been proved, the next task is to evolve a suitable engine-test technique for rating lubricating oils which will accurately predict their performance in service. This programme, organized and supervised by the Engine Tests of Lubricants Panel of the Institute of Petroleum, will demand the fullest co-operation from both oil companies and the diesel-engine manufacturers and users.

CALIBRATION OF I.P. DIESEL REFERENCE FUELS H.I.Q. AND L.I.Q. IN TERMS OF CETANE NUMBER.

DURING 1937 the Ignition Quality of Diesel Fuels Panel of Standardization Sub-Committee No. 5—Engine Tests—made arrangements to adopt common secondary reference fuels in the United Kingdom for the use of laboratories testing diesel fuels. The Anglo-Iranian Oil Company, Ltd., undertook to manufacture two such fuels designated High-Ignition-Quality (H.I.Q.) and Low-Ignition-Quality (L.I.Q.) reference fuels respectively. Calibration tests against primary fuels (cetane and alpha-methylnaphthalene) were carried out in three laboratories on four types of engines. The results of this calibration were published * and showed that the H.I.Q. had a cetane number of 70½, and the L.I.Q. a cetane number of 18.

The I.P. reference fuels were in limited use in the U.K. during the War, but there was little opportunity for different laboratories to compare results. It therefore seemed desirable to the Panel to undertake a re-check of the calibration and this was completed during 1948. The necessary engine-test facilities were only available in seven laboratories and covered five types of engines. The A.S.T.M. method D613–43(T) standardizes the C.F.R. diesel engine for cetane ratings, but only three of these were available among the engines used. I.P. Method No. 41 accepts the A.S.T.M. procedure and describes two alternative methods which can be applied to a range of suitable engine types. One of these methods depends on measurement of the changes in ignition lag in the cylinder, and the other uses a throttling device whereby the supply of air to the engine is restricted progressively until misfire occurs.

Supplies of the primary reference fuels required for a re-calibration were strictly limited, and it was known that there was a possibility of slight variations in purity between different consignments of alpha-methylnaphthalene. Fortunately the Anglo-Iranian Oil Co., Ltd., had available sufficient of both the primary fuels to supply all the participating laboratories, and they kindly offered to distribute four blends of primary fuels for the purpose of the co-operative tests. These blends were designated W, X, Y, and Z and actually contained 28, 39, 50, and 61 per cent cetane respectively.

Co-operating laboratories were asked to rate these blends on their engines in terms of the composition of a matching blend of the I.P. secondary reference fuels, using as many alternative approved methods as possible. The results are summarized in Table I.

As would be expected with such diversified tests the figures show appreciable spread. Careful examination of the results led the Panel to conclude that there was no consistent trend in the observed differences between engines or methods. It was therefore decided to accept the arithmetic mean of the results, and the data thus obtained are compared in Table II with the previous calibration.

---

* *J. Inst. Petrol. Techn.*, 1938, **24**, 170.

TABLE I.

Laboratory.	Engine.	Method.	Per cent I.P. high in low to match fuel.			
			W.	X.	Y.	Z.
A	C.F.R.	A.S.T.M.	16·9	43·3	62·8	79·7
	Gardner	Delay	13·7	35·0	55·4	78·0
	Gardner	Throttling	13·2	33·0	59·0	83·7
B	C.F.R.	A.S.T.M.	21·3	39·4	54·5	75·7
C	A.E.C.	Delay	16·0	35·8	59·5	80·0
		Throttling	16·0	35·5	59·0	80·3
D	Gardner	Throttling	—	32·8	61·9	83·3
E	Gardner	Throttling	13·8	37·2	59·0	—
F	Crossley	Throttling	—	41·9	65·6	75·2
	C.F.R.	Throttling	18·0	41·9	63·0	80·0
G	I.G.	Var. comp. 18° delay	17·0	38·5	61·1	81·1
		Average	16·2	37·7	60·1	79·7
		Spread	8·1	10·5	11·1	8·5

TABLE II.

Blend.	Cetane, per cent.	Per cent H.I.Q. in L.I.Q.		Difference.
		1938 calibration.	1948 calibration.	
W	28	19	16·2	2·8
X	39	40	37·7	2·3
Y	50	61	60·1	0·9
Z	61	82	79·7	2·3

A difference of 1 per cent in the composition of the matching blend of secondary fuels is equivalent to 0·53 cetane number. Whilst the 1948 results suggest that a given cetane number was obtained with a slightly lower percentage of H.I.Q. in the matching blend than was the case in 1938, the difference is in all cases within the limits of experimental error. It was therefore decided by the Panel that there was insufficient evidence to justify any change from the original calibration and, until it is possible to include more engines, the earlier conclusion holds, namely: that the cetane number of H.I.Q. reference fuel is 70½ and L.I.Q. reference fuel 18 and that the calibration is a straight line.